

Wavelet-Based Separating Kernels for Array Processing of Cellular DS/CDMA Signals in Fast Fading

Massimiliano (Max) Martone, *Member, IEEE*

Abstract—We propose new detectors for direct-sequence code-division multiple-access (CDMA) signals that outperform known approaches in rapidly fading multipath channels. Multipath compensation in CDMA systems is a problem of significant complexity especially when rapidly fading is afflicting the radio frequency channel. In this work, we depart from typical approaches in search of new kernels that can more accurately characterize the time-varying nature of the estimation problem and focus on a multiresolution representation of the fading processes. The unknown channel time variations are in fact decomposed using optimal unconditional bases in the family of the orthonormal wavelets. We show that it is possible to represent the channel in a reduced-order dimensional space by matching the scattering function of the multipath channel to its decomposition and obtain an approach that is effective in fast fading environments, such as those practically found in macrocell wireless communication applications. We apply this representation to the development of a practical multiscale filter that achieves multiuser separation minimizing a time-averaged squared error. The technique is studied by means of computer simulations and hardware experiments that employ a currently deployed base-station system.

Index Terms—Array signal processing, code-division multiple-access, interference suppression, land mobile radio cellular systems.

I. INTRODUCTION

THE performance of code-division multiple-access (CDMA) systems is severely degraded by frequency-selective multipath radio frequency (RF) propagation. The mitigation of this effect based on the use of multiuser/multi-antenna detectors has attracted significant interest in recent years. The crucial point of almost all of the proposed methods is based on the assumption that the multipath channels are quasi-static, that is, time invariant over the length of the transmitted frame. Slow variations of the channels are then compensated by using adaptive algorithms that ultimately force the estimate to be constantly in search of a convergence point. If the channel coefficients variations in time are fast with respect to the convergence time of the adaptive algorithm, significant degradation may result. A more reasonable alternative is to model the time-varying components of the impulse response

of the multipath channel as low-pass Gaussian processes with their correlation representing ensemble average characteristics. These average characteristics are in turn used to fit parametric models so that a bank of Kalman filters can be used for tracking. This approach is impractical because the parametric models that best fits the channel dynamics have a large number of free parameters [2], [23]. Moreover, the generalization of this approach to a multiuser environment where possibly multiple different channel responses have to be estimated/tracked is definitely a formidable task in terms of computational effort. In this work, we depart from these well-known and obvious approaches in search of new methods that more “economically” can characterize the time-varying nature of the detection/estimation problem, and we focus on a multiresolution representation of the fading process in each component of the channel response, elaborating some ideas of [26], [31], [6], [11] (and in a sense [9]) as they apply to the direct-sequence CDMA (DS/CDMA) detection problem. The unknown channel time variations are in fact decomposed using optimal unconditional bases [7] such as orthonormal wavelet bases [4], [5]. The use of basis expansion models in the representation of time-varying multipath channels is discussed in [9], but was used in earlier works on multipath modeling [3]. It is extremely important to realize that modeling of linear systems by basis functions can turn a time-varying system identification problem into a time-invariant one. Essentially inspired by Fourier harmonic analysis ideas, simple exponential bases were used in [9]. The exponential basis function of a Fourier-like decomposition has infinite duration, so clearly any representation of a time-localized signal is not efficient and adequate. To connect this consideration with a simple and intuitive example, consider a signal made of two pure oscillations occurring at nonoverlapping distinct time intervals. The Fourier transform (FT) reveals the presence of the two tones, but with no localization in time, which forces a wrong representation for the signal. In other words, representations based on exponentials lack “parsimony.” The time-varying reflections of electromagnetic waves caused by a moving transmitter (or receiver) are in nature very similar to a signal where multiple propagation modes are present at different times. To represent the frequency behavior of a signal locally in time, the signal should be analyzed by functions which are localized both in time and frequency, for instance, signals that are compactly supported in the time and frequency domains. In reality, no function can be compactly supported simultaneously in time and frequency, so the scientific community

Paper approved by Z. Kotic, the Editor for Wireless Communication of the IEEE Communications Society. Manuscript received December 29, 1998; revised May 10, 1999 and July 26, 1999.

The author was with the Telecommunications Group, Watkins-Johnson Company, Gaithersburg, MD 20878-1794 USA. He is now with WJ Communications, Palo Alto, CA 94304-1204 USA.

Publisher Item Identifier S 0090-6778(00)05399-X.

has directed intense research efforts in the development of functions with “good” time-frequency localization: wavelets are the best known tool for linear time-frequency analysis. Another example of multipath modeling using harmonic decompositions is also contained in [10], where the problem of needing a large number of exponentials for a reasonable accuracy was also emphasized. Many more considerations regarding the disadvantages of Fourier analysis in practical problems can be found in [8] and [7]. An obvious solution to the time-localization problem of the Fourier analysis is to localize the tones in the Fourier representation by windowing several time-consecutive intervals of the analyzed signal. This is, in fact, the short-time FT which basically operates a partition (or “tiling”) of the time-frequency plane in rectangles of equal area. Wavelets can offer a different and valuable compromise: the frequency localization is logarithmic in frequency. Looking at the time-frequency plane, this means that time localization gets finer at the highest frequencies. The wavelet transform replaces the FT’s sinusoidal waves by a family of functions generated by translations and dilations of a single window called a wavelet. Complicated signals can be represented using only a few wavelet and scaling functions, and statistical signal modeling and processing methods based on the wavelet transform are in most cases much more effective than classical time-domain or frequency-domain approaches.

A. Significance of Modeling Time-Varying Systems Using Wavelets

In this section, we give a brief explanation of the ideas contained in this paper by using an oversimplified continuous-time single-user model. Consider a sequence of symbols collected in the vector \mathbf{a} , digitally modulated to form the signal $x(t, \mathbf{a})$. The signal $x(t, \mathbf{a})$ is input to $h(t, \tau)$, the time-varying impulse response of a multipath channel, as

$$y(t) = \int_{-\infty}^t h(t, t - \tau) x(\tau, \mathbf{a}) d\tau. \quad (1)$$

Assume that the kernel $h(t, \tau)$ can be represented by an expansion of the form

$$h(t, \tau) = \sum_{I \in \mathcal{I}_h} w_I(\tau) \psi_I(t) \quad (2)$$

where $\{\psi_I(t)\}_{I \in \mathcal{I}_h}$ is a set of functions (wavelets) and $\{w_I(\tau)\}_{I \in \mathcal{I}_h}$ are the (wavelet) coefficients of the expansion. Using this representation, we can express (1) as

$$y(t) = \sum_{I \in \mathcal{I}_h} \psi_I(t) \int_{-\infty}^t w_I(t - \tau) x(\tau, \mathbf{a}) d\tau = \sum_{I \in \mathcal{I}_h} \psi_I(t) \tilde{x}_I(t, \mathbf{a}) \quad (3)$$

where $\tilde{x}_I(t, \mathbf{a}) = \int_{-\infty}^t w_I(t - \tau) x(\tau, \mathbf{a}) d\tau$. This representation can be economical if the set $\{\psi_I(t)\}_{I \in \mathcal{I}_h}$ contains a small number of functions. The multiplication $\psi_I(t) \tilde{x}_I(t, \mathbf{a})$ emphasizes the time selection of the input content and its frequency translations. Observe that $\tilde{x}_I(t, \mathbf{a})$ for any I in the set \mathcal{I}_h is the output of a time-invariant linear filtering operation: it is simply

obtained filtering $x(t, \mathbf{a})$ by $w_I(t)$. Another interesting property of this representation is that it gives us the ability to select for any given time interval only those wavelet coefficients responses $w_I(\tau)$ that affect the output during the time interval of interest. Assume now that white Gaussian noise $n(t)$ afflicts the channel output as $\tilde{y}(t) = y(t) + n(t)$. The maximization of the likelihood function with respect to the transmitted sequence of symbols \mathbf{a} is easily seen to be equivalent to the maximization of the function [28]

$$L_{\mathcal{T}}(\mathbf{a}) = - \int_{t \in \mathcal{T}} \left| \tilde{y}(t) - \int_{\tau \in \mathcal{T}} h(t, t - \tau) x(\tau, \mathbf{a}) d\tau \right|^2 dt \\ = - \int_{t \in \mathcal{T}} \left| \tilde{y}(t) - \sum_{I \in \mathcal{I}_h} \psi_I(t) \tilde{x}_I(t, \mathbf{a}) \right|^2 dt \quad (4)$$

where \mathcal{T} is the time interval over which we observe $\tilde{y}(t)$ and $\tilde{x}_I(t, \mathbf{a}) = \int_{\tau \in \mathcal{T}} w_I(t - \tau) x(\tau, \mathbf{a}) d\tau$. The wavelet-based representation gives the possibility of an economical, but still accurate, formulation of the optimal detector based on the maximization of (4). In fact, it is possible to select a subset of the functions and coefficients in \mathcal{I}_h such that $\int_{\tau \in \mathcal{T}} h(t, t - \tau) x(\tau, \mathbf{a}) d\tau$ is well represented only over the time interval \mathcal{T} . This is quite valuable and somehow impossible using known nontime localized models. We have already presented an application of this maximum-likelihood (ML) time-localized approach to ML sequence estimation detection of narrow-band digital signals in [15]. Unfortunately, we will find that the application of this idea to a multiuser system is very demanding in terms of computational complexity, so we will turn our attention to a simplified linear detector, one that is based on the design $g(t, \tau)$ that is expanded onto the same wavelet basis used in the channel model and whose coefficients minimize an averaged squared error

$$M_{\mathcal{T}}[g(t, \tau)] = \int_{t \in \mathcal{T}} \left| x(t, \mathbf{a}) - \int_{\tau \in \mathcal{T}} g(t, t - \tau) \tilde{y}(\tau) d\tau \right|^2 dt \\ = \int_{t \in \mathcal{T}} \left| x(t, \mathbf{a}) - \sum_{I \in \mathcal{I}_g} \psi_I(t) \tilde{y}_I(t) \right|^2 dt \quad (5)$$

where $\tilde{y}_I(t) = \int_{-\infty}^t w_{g,I}(t - \tau) \tilde{y}(\tau) d\tau$. Again, the wavelet-based representation gives the possibility of an economical, but still accurate, design of a time-varying filter by means of a selection of a subset of functions and coefficients in \mathcal{I}_g such that $\int_{\tau \in \mathcal{T}} g(t, t - \tau) \tilde{y}(\tau) d\tau$ is well represented over the time interval \mathcal{T} .

The use of wavelet bases allows the selection of the subset in \mathcal{I}_h (or \mathcal{I}_g), which will model the *local* and *global* characteristics of the channel dynamics. A clear attempt of the engineering community to have a global characterization of the time-varying nature of a multipath propagation link is the well-known wide-sense stationary uncorrelated scattering (WSSUS) model [21]. The WSSUS assumption is only an approximation of the real propagation mechanism in a dense multipath environment. Indeed, $h(t, \tau)$ has smooth (low frequency) variations with occasional rapid changes that cannot be possibly modeled as stationary. In particular, a channel model which is uniquely

based on ensemble average characteristics will inevitably lose local characteristics that are caused, for example, by rapid transitions and sudden changes of the impulse response dynamics (for example, the mobile transmitter coming to a sudden stop), while the multiresolution model will retain such information in a few high-resolution *detail* coefficients. The idea that the wavelet-based representations can better model not only non-stationary but also stationary processes is also the motivation for [31] and [6]. We will however use the WSSUS model to tune our channel representation and to eliminate gross redundancy; in other words, second-order statistics will provide general guidelines on how to select the low-resolution coefficients. It is however understood that retaining only the low-resolution coefficients will not give us the kind of “parsimony” that we expect from a wavelet-based representation. To achieve this goal, a few high-resolution coefficients empirically selected will be maintained.

The paper is organized as follows. In Section II, we give a brief introduction to wavelet-based signal processing methods. In Section III, we review the CDMA system model, and in Section IV, we study the channel basis expansion. In Section V, we motivate a reasonable reduced dimensional representation of the fading channel. In Section VI, we present possible approaches to detection with a practical time-variant filter, also implemented as an adaptive filter. In Section VII, the results of simulations and hardware experiments are shown.

II. DISCRETE WAVELET TRANSFORMATIONS

A generic signal $f(t)$ can be represented in terms of translates and dilates of a single prototype (typically bandpass) wavelet $\psi(t)$

$$f(t) = \sum_{l,m=-\infty}^{+\infty} \xi(l,m) 2^{-l/2} \psi(2^{-l}t - m) \quad (6)$$

or equivalently for some $P > 0$

$$f(t) = \sum_m \zeta(m) 2^{-P/2} \phi(2^{-P}t - m) + \sum_{l=-\infty}^P \sum_m \xi(l,m) 2^{-l/2} \psi(2^{-l}t - m) \quad (7)$$

where

$$\xi(l,m) = \int_{-\infty}^{+\infty} f(t) 2^{-l/2} \psi(2^{-l}t - m) dt$$

are wavelet (or *detail*) coefficients

$$\zeta(m) = \int_{-\infty}^{+\infty} f(t) 2^{-P/2} \phi(2^{-P}t - m) dt$$

are scaling (or *approximation*) coefficients, and $\phi(t)$ is a low-pass scaling function [4], [5]. Particularly important is the interpretation of (7) as a multiresolution analysis of $f(t)$: l indexes the *scale*, or *resolution* (the smaller l the higher the resolution), while m indexes the *spatial* location of analysis. If the mother wavelet is centered at time 0 and frequency f_c , $\xi(l,m)$ measures the content of $f(t)$ around time $2^l m$ and

frequency $2^{-l} f_c$, while $\zeta(m)$ represents the local mean around time $2^P m$. In this framework, we can think of $f(t)$ as the finest scale ($P = 0$) representation of $f(t)$ itself. The function $\psi(t)$ has to satisfy some critical conditions to ensure that (7) holds for any square integrable function $f(t)$. In particular, $\psi(t)$ has to satisfy the two scale equations

$$\phi(t) = \sqrt{2} \sum_n c_0(n) \phi(2t - n) \quad (8)$$

$$\psi(t) = \sqrt{2} \sum_n c_1(n) \phi(2t - n) \quad (9)$$

where the coefficients $c_i(n)$ can be nonzero¹ only over a finite number of consecutive values of n . Define $\psi_{l,m}(t) = 2^{-l/2} \psi(2^{-l}t - m)$ and $\phi_{l,m}(t) = 2^{-l/2} \phi(2^{-l}t - m)$. The three orthogonalities constraints imposed are **O1**: $\int \phi_{l,m}(t) \phi_{l,m'}(t)^* dt = \delta(m - m')$, **O2**: $\int \psi_{l,m}(t) \psi_{l,m'}(t)^* dt = \delta(m - m') = \delta(l - l')$, and **O3**: $\int \psi_{l,m}(t) \phi_{l,m'}(t)^* dt = \delta(m - m') = 0$. It is possible to show that **O1**, **O2**, **O3** are satisfied by coefficients $c_i(n)$ that have the following properties:

$$\sum_n c_0(n) c_0(n + 2k) = \delta(k)$$

$$c_1(n) = (-1)^n c_0(n).$$

A remarkable observation can be made: $c_i(n)$ are the coefficients of a perfect reconstruction two-band (or dyadic) filter bank with the quadrature mirror reconstruction property [27]. Therefore, the design of wavelets is equivalent to the design of filter banks. Observe that the conditions imposed up until now are not sufficient to construct in practice useful wavelets. In fact, they can lead to decompositions with not enough regularity. Regularity is imposed requiring a large number of vanishing moments [4], [5]. In practice, $\zeta(m)$ and $\xi(l,m)$ can be computed **recursively** from $\xi(l+1,m)$ using the efficient pyramid algorithm proposed by Mallat in [14]. It is not necessary to explicitly compute the shape of $\phi(t)$ and $\psi(t)$. The basic application of wavelets in this paper stems from a multiresolution decomposition [which simply specializes the expansion in (2)] of a time-varying multipath response of the form $\tilde{h}(t,\tau)$ at any τ with respect to t as

$$\tilde{h}(t,\tau) = \sum_m \zeta(m,\tau) 2^{-P/2} \phi(2^{-P}t - m) + \sum_{l=-\infty}^P \sum_m \xi(l,m,\tau) 2^{-l/2} \psi(2^{-l}t - m) \quad (10)$$

where $\xi(l,m,\tau)$ are wavelet coefficients and $\zeta(m,\tau)$ are scaling coefficients. If the channel is modeled as deterministic, wavelet and scaling coefficients are considered deterministic, and if the channel is modeled as random, wavelet and scaling coefficients are considered random parameters. The wavelet-based representation will exhibit *global* characteristics of the channel dynamics in the low-resolution coefficients,

¹By doing so, we restrict our description to compactly supported wavelets [27].

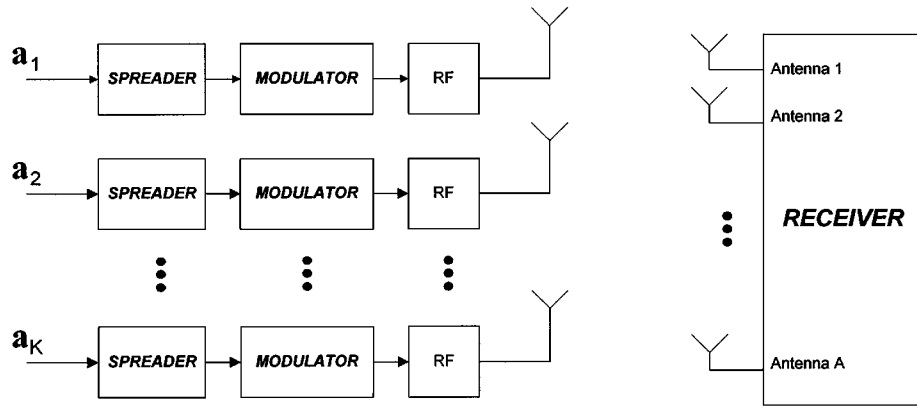


Fig. 1. System model in the uplink of a cellular system.

while retaining *local* rapid transitions in just a few coefficients at higher resolutions. A practical advantage is that the decomposition decouples the variations in time and relegates them in $\psi(t)$ and $\phi(t)$, so that the wavelets coefficients are indeed time invariant for any τ . Moreover, since we will assume discretized responses with resolvable multipath components of the form $\tilde{h}(t, \tau) = \sum_{l=1}^Q f_l(t)\delta(\tau - \tau_l)$, we will significantly simplify (10).

III. SYSTEM MODEL

In this section, we briefly review the system model for the reverse link of a CDMA cellular system. No particular assumption is made on the geometry of the array at the base station, and we intentionally neglect the propagation assumptions of the model. More details regarding these assumptions can be found in [16], [18], and [17]. In a DS/CDMA communication system [13], the information signal relative to the k th user is given by

$$m_k(\tau) = \sum_{n=0}^{M-1} a_k(n) p_{T_s}(\tau - nT_s), \quad k = 1, 2, \dots, K \quad (11)$$

where

$$p_{\tilde{\tau}}(\tau) = \begin{cases} 1, & \text{if } 0 < \tau < \tilde{\tau} \\ 0, & \text{otherwise} \end{cases}$$

and $\mathbf{a} = \{a_k(n)\}_{n=1}^M$ is the real or complex message (to include any type of digital modulation scheme) composed of \tilde{m} -ary symbols of duration T_s . The K users *asynchronously* share the common channel using the signatures waveforms

$$a_{c,k}(\tau) = \sum_{n=1}^J a_{c,n}^k p_{T_c}(\tau - nT_c), \quad k = 1, 2, \dots, K \quad (12)$$

where $T_c = T_s/J$ is the chip period and $\{a_{c,n}^k \in (-1; +1)\}_{n=1}^J$ is the pseudonoise (PN) spreading sequence of length J . The spreading signal waveform (12) of the k th user has duration T_s and is normalized to unit power. If an equivalent low-pass representation is employed, the k th transmitted spread-spectrum signal can be written as $\sum_{i=0}^{M-1} a_k(i) p_{T_s}(\tau - iT_s) a_{c,k}(\tau - iT_s)$. This signal is distorted by multipath RF propagation and multiple-access interference caused by other RFs. Each mobile

transmitter has a single antenna (see Fig. 1), while at the base station, the multiplexed signal is received through an A -sensor antenna. The received signal at the base-station receiver can be represented² as

$$r^\kappa(t) = \sum_{i=0}^{M-1} \sum_{k=1}^K a_k(i) \sqrt{E_k^s(i)} \tilde{f}_k^\kappa(t, t - iT_s) + n^\kappa(t), \quad \kappa = 1, 2, \dots, A \quad (13)$$

where $\tilde{f}_k^\kappa(t, \tau) = e^{j\theta_k} a_{c,k}(\tau) * \tilde{h}_k^\kappa(t, \tau)$ ($*$ denotes convolution) is the combined impulse response of each signal path of the k th spreading waveform and the channel from the k th user to the κ th sensor, and $E_k^s(i)$ and θ_k are the received signal power and the carrier phase of the k th transmitted signal relative to the k th user, respectively. The channel $\tilde{h}_k^\kappa(t, \tau)$ between the k th transmitter and the κ th sensor for $k = 1, 2, \dots, K$ and $\kappa = 1, 2, \dots, A$ is

$$\tilde{h}_k^\kappa(t, \tau) = \sum_{l=1}^Q f_{k,l}^\kappa(t) \delta(\tau - \tau_{k,l}^\kappa). \quad (14)$$

$f_{k,l}^\kappa(t)$ are the normalized fading complex envelope processes so that $E_k^s(i)$ reflects the k th user received energy over the time period corresponding to iT_s , and $\delta(n)$ is the delta function. The noise in (13) is white Gaussian, with two-sided power spectral density $N_0/2$; it can also represent the surrounding cell interference, plus noise. Multipath channels enhance interference among users, introducing intersymbol interference and additional correlation between the spreading waveforms. Received energies are assumed invariant over the duration of the message: $E_k^s(i) = E_k^s$ for $i = 0, \dots, M-1$. We assume that the receiver has perfect knowledge of the powers, time delays $\tau_{k,l}^\kappa$, and phase lags of every received user signal. At the receiver, a bank of KQ filters for each sensor (see Figs. 2 and 3), each filter matched to

²Equation (13) with (12) assumes the code remains the same from bit to bit for a particular user. However, IS-95 and many other CDMA systems use different parts of a longer code for each bit. Besides substituting $a_{c,k}^{(i)}(\tau)$, where now the code utilized by the k th user depends on the bit index (i), the rest of the signal model is still valid for systems using long codes (defined aperiodic systems in [29]). For simplicity of exposition, we limit our model description to periodic systems. Since the same multichannel model (16) can be derived for the aperiodic (long codes) case, the presentation of the algorithms that follow also apply to practical CDMA systems like third-generation (3G)-CDMA and IS-95.

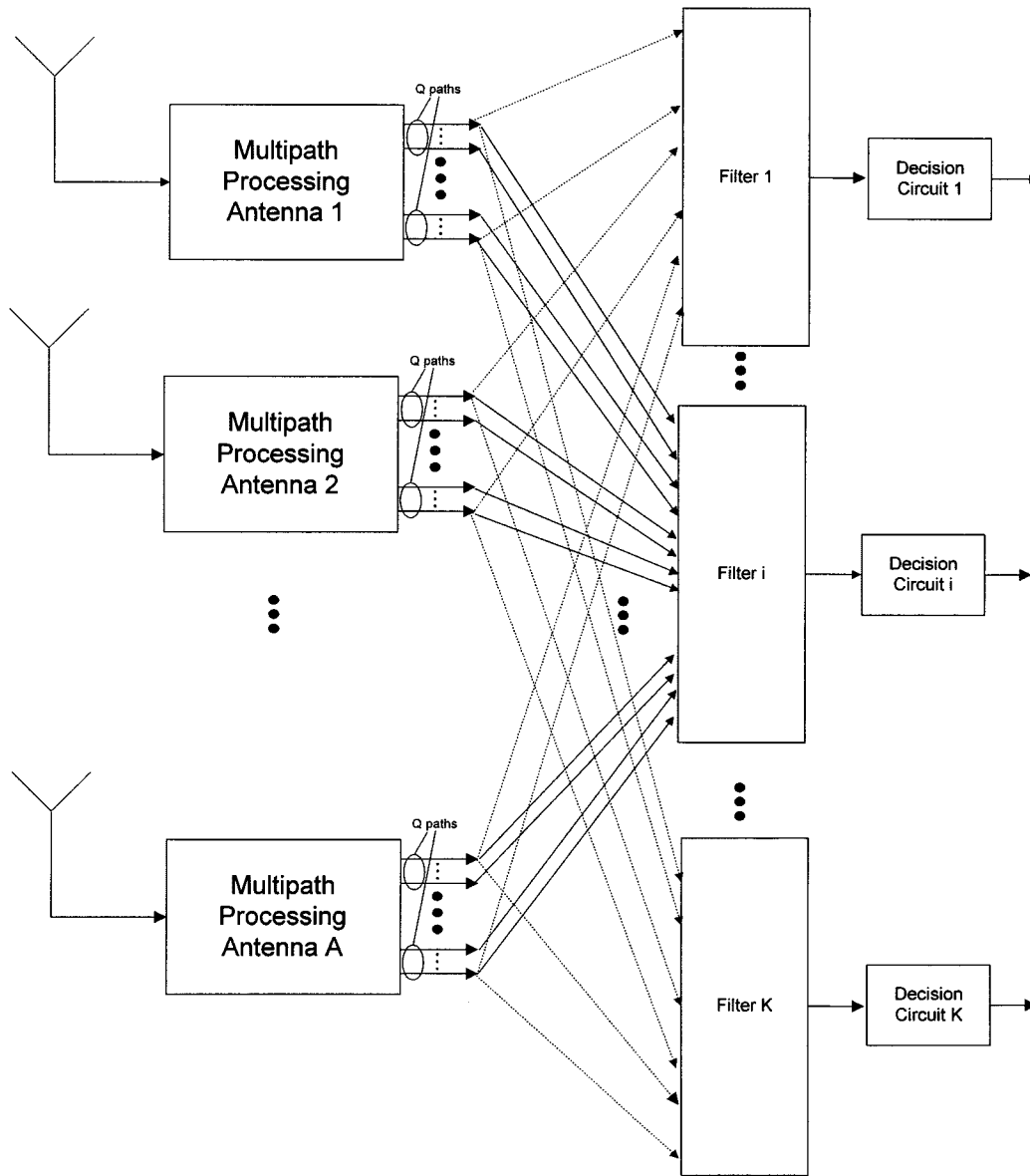


Fig. 2. Architecture of the receiver.

a delayed replica of the wanted spread-spectrum signature, performs despreading with the signatures in (12) and is sampled at symbol rate to obtain the set of samples

$$y_{k,l}^{\kappa}(n) = \int_{nT_s}^{(n+1)T_s} r^{\kappa}(\tau) a_{c,k}(\tau - nT_s - \tau_{k,l}^{\kappa}) d\tau. \quad (15)$$

The input/output relation for the multichannel discrete-time system can be written as

$$\begin{aligned} y_{i,l}^{\kappa}(n) &= \sum_{k=1}^K \sum_{q=1}^Q \sum_m \bar{h}_{i,k,l,q}^{\kappa}(n,m) a_k(n-m) + \eta_{i,l}^{\kappa}(n) \\ &= \sum_{k=1}^K \sum_m h_{i,k,l}^{\kappa}(n,m) a_k(n-m) + \eta_{i,l}^{\kappa}(n), \\ i &= 1, 2, \dots, K; \kappa = 1, 2, \dots, A; l = 1, 2, \dots, Q \end{aligned} \quad (16)$$

where

$$\begin{aligned} \bar{h}_{i,k,l,q}^{\kappa}(n,m) &= \sqrt{E_k^s} e^{j\theta_k} f_{k,q}^{\kappa}(nT_s) \\ &\quad \times \int_{-\infty}^{+\infty} a_{c,i}(u - \tau_{i,l}^{\kappa}) a_{c,k}(u + mT_s - \tau_{k,q}^{\kappa}) du \\ h_{i,k,l}^{\kappa}(n,m) &= \sum_{q=1}^Q \bar{h}_{i,k,l,q}^{\kappa}(n,m) \end{aligned} \quad (17)$$

and $\eta_{i,l}^{\kappa}(n)$ is the noise component.

IV. WAVELET-BASED CHANNEL BASIS EXPANSION

We would like to obtain a practical basis representation for the discrete-time channel $h_{i_1, i_2, i_3}^{\kappa}(n, k)$ that is easily parametrized, it retains the essential features of the fading process and it characterizes these features using a small number of time-invariant coefficients. These requirements can be satisfied using a

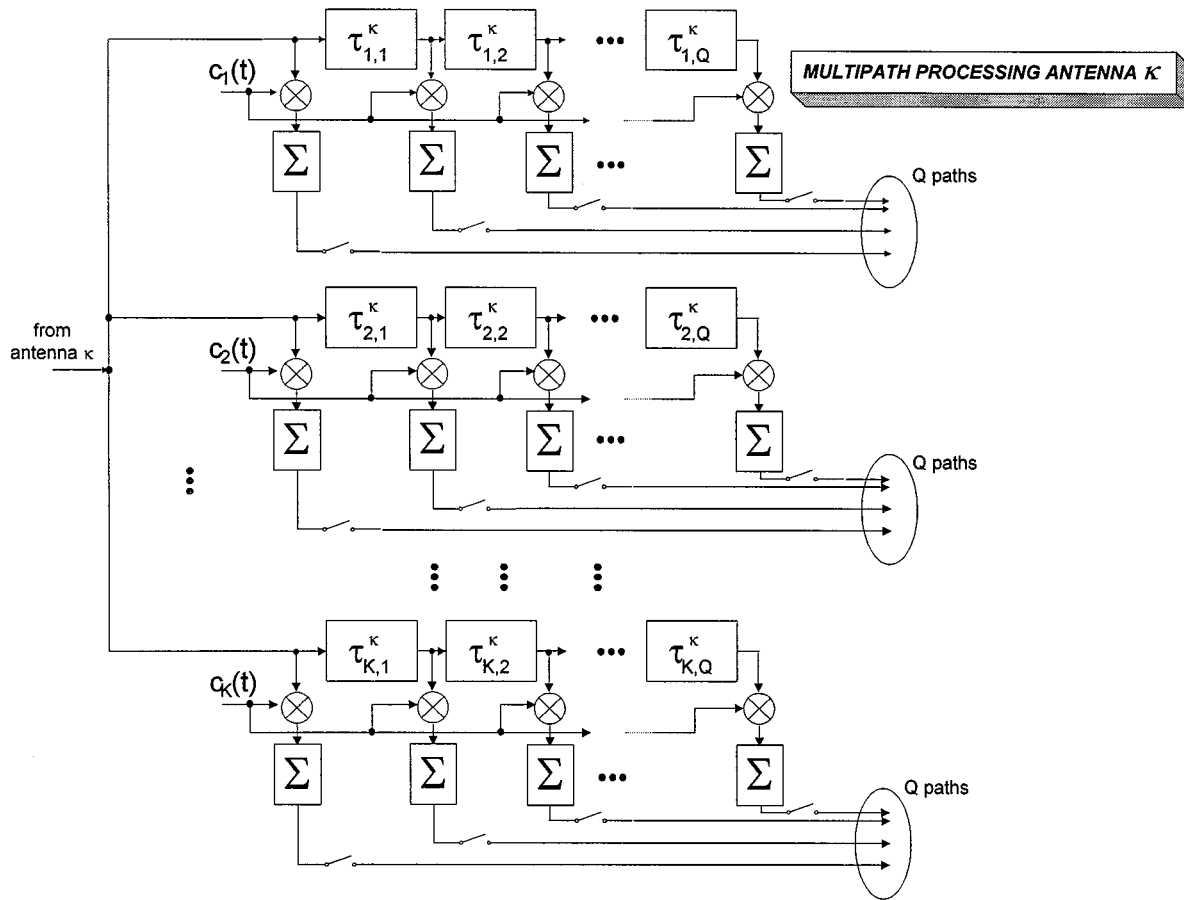


Fig. 3. Signal processing subsection relative to antenna κ .

discrete-time wavelet series representation. An important technical aspect arises. We do not need the coefficients of the continuous-time wavelet series expansion of

$$\begin{aligned} \tilde{h}_{i,k,l,q}^{\kappa}(t, \tau) &= \sum_{q=1}^Q \sqrt{E_k^s} e^{j\theta_k} f_{k,q}^{\kappa}(t) \\ &\times \int_{-\infty}^{+\infty} a_{c,i}(u - \tau_{i,l}^{\kappa}) a_{c,k}(u + \tau - \tau_{k,q}^{\kappa}) du \end{aligned} \quad (18)$$

to obtain a representation of the form in (10). We only need a discrete-time wavelet series representation of a sampled version of $\tilde{h}_{i,k,l,q}^{\kappa}(t, \tau)$, that is $h_{i_1, i_2, i_3}^{\kappa}(n, k) = \tilde{h}_{i,k,l,q}^{\kappa}(t, \tau)|_{t=nT_s, \tau=mT_s}$. It is possible to show that for a high resolution (that is large P) and short T_s , the discrete-time series coefficients and continuous-time series coefficients asymptotically converge to the same values. The orthonormal expansion we will derive can be thought more properly as a multiscale subband decomposition using filterbanks of the sampled response of a multipath channel. We direct the interested reader to [27] and in particular to [22], where a “discrete-time” approach to multiresolution representations is described.

To simplify notation, consider $h(n, k)$ as the generic response for a generic set of indices κ, i_1, i_2, i_3 . It is fundamental to observe that $h(n, k)$ can be represented at lower resolution

applying a half-band low-pass filter having impulse response $c_0(n)$, followed by a downsampling-by-two operation

$$\zeta_{1,m}(k) = \sum_l c_0(l) h(2m - l, k). \quad (19)$$

This equation represents a mapping from a vector space to itself. An added “detail” can be obtained by using a high-pass filter with impulse response $c_1(n)$, then again downsampling by two

$$\xi_{1,m}(k) = \sum_l c_1(l) h(2m - l, k). \quad (20)$$

The filters $c_i(n)$ $i = 0, 1$ satisfy some regularity constraints [4], [5] and form an orthonormal set. If $c_i(n)$ in the z -domain $C_i(z)$ $i = 0, 1$ is a dyadic perfect reconstruction filter bank [27], one can think of (19) and (20) as a *decomposition* of $h(n, k)$ onto a discrete-time orthonormal basis with the following (perfect) reconstruction rule:

$$h(n, k) = \sum_{m=0}^{N/2-1} \zeta_{1,m}(k) c_0(2m - n) + \sum_{m=0}^{N/2-1} \xi_{1,m}(k) c_1(2m - n) \quad (21)$$

which is indeed a sum of orthogonal projections. Using the same filters $c_0(m), c_1(m)$, (19) could be split again in low-pass and high-pass downsampled components, and then the low-pass component could be further split again to a desired “depth” or

resolution, so that one can always “explode” the low-pass component resolution

$$\zeta_{l,n}(k) = \sum_{m=0}^{N/2-1} \zeta_{l+1,m}(k)c_0(2m-n) + \sum_{m=0}^{N/2-1} \xi_{l+1,m}(k)c_1(2m-n). \quad (22)$$

For example, consider (22) for $l = 1$ and substitute in (21) to get

$$\begin{aligned} h(n,k) &= \sum_{m=0}^{N/2-1} \left[\sum_{m'=0}^{N/2-1} \zeta_{2,m'}(k)c_0(2m'-m) + \sum_{m'=0}^{N/2-1} \xi_{2,m'}(k)c_1(2m'-m) \right] c_0(2m-n) \\ &+ \sum_{m=0}^{N/2-1} \xi_{1,m}(k)c_1(2m-n) \\ &= \sum_{m=0}^{N/2^2-1} \zeta_{2,m}(k)c_0^{(2)}(2^2m-n) \\ &+ \sum_{l=1}^2 \sum_{m=0}^{N/2^l-1} \xi_{l,m}(k)c_1^{(l)}(2^lm-n) \end{aligned} \quad (23)$$

where $c_0^{(2)}(n)$, $c_1^{(1)}(n)$, and $c_1^{(2)}(n)$ are filters obtained in the z -domain as $C_0^{(2)}(z) = C_0(z)C_0(z^2)$, $C_1^{(1)}(z) = C_1(z)$, $C_1^{(2)}(z) = C_1(z^2)C_0(z)$. In the last equation, we have used the Noble identity [27] which says that a downsampler by two, followed by a filter $F(z)$, is equivalent to the filter $F(z^2)$ followed by the downsampler by two. We can think of (23) as a decomposition of $h(n,k)$ onto a discrete-time orthonormal basis at resolution level $P = 2$. The method can be applied recursively to obtain at generic resolution depth P a filter bank with $P + 1$ branches

$$\begin{aligned} h(n,k) &= \sum_{m=0}^{N/2^P-1} \zeta_{P,m}(k)c_0^{(P)}(2^Pm-n) \\ &+ \sum_{l=1}^P \sum_{m=0}^{N/2^l-1} \xi_{l,m}(k)c_1^{(l)}(2^lm-n) \end{aligned} \quad (24)$$

where $\zeta_{P,m}(k)$ and $\xi_{l,m}(k)$ are coefficients of the wavelet-based decomposition (WBD), and the filters $c_0^{(P)}(n)$ and $c_1^{(l)}(n)$ (with real coefficients) are given in the z -domain by

$$\begin{aligned} C_0^{(P)}(z) &= \prod_{i=0}^{P-1} C_0(z^{2^i}) \\ C_1^{(l)}(z) &= C_1(z^{2^{l-1}}) \prod_{i=0}^{l-2} C_0(z^{2^i}). \end{aligned} \quad (25)$$

The expression (24) with (25) can be easily obtained making use of the Noble identities [27]. This approach essentially uses a binary subband tree structure that is constructed using

stages of two-channel filterbanks [27]. Specializing (24) to $h_{i_1,i_2,i_3}^{\kappa}(n,k)$, we have

$$\begin{aligned} h_{i_1,i_2,i_3}^{\kappa}(n,k) &= \sum_{m=0}^{N/2^P-1} \zeta_{P,m,i_1,i_2,i_3}^{\kappa}(k)c_0^{(P)}(2^Pm-n) \\ &+ \sum_{l=1}^P \sum_{m=0}^{N/2^l-1} \xi_{l,m,i_1,i_2,i_3}^{\kappa}(k)c_1^{(l)}(2^lm-n) \end{aligned} \quad (26)$$

where $\zeta_{P,m,i_1,i_2,i_3}^{\kappa}(k)$ and $\xi_{l,m,i_1,i_2,i_3}^{\kappa}(k)$ are discrete wavelet transform (DWT) coefficients. Using vector notation, it is possible to express (26) simply as

$$h_{i_1,i_2,i_3}^{\kappa}(n,k) = \mathbf{c}(P,n)^T \mathbf{w}_{i_1,i_2,i_3}^{\kappa}(P,k) \quad (27)$$

where the organization of the wavelet coefficients in $\mathbf{w}_{i_1,i_2,i_3}^{\kappa}(P,k)$ is

$$\begin{aligned} \mathbf{w}_{i_1,i_2,i_3}^{\kappa}(P,k) &= [\zeta_{P,i_1,i_2,i_3}^{\kappa}(k)^T \zeta_{1,i_1,i_2,i_3}^{\kappa}(k)^T \cdots \zeta_{P,i_1,i_2,i_3}^{\kappa}(k)^T]^T \end{aligned}$$

with³

$$[\zeta_{P,i_1,i_2,i_3}^{\kappa}(k)]_m = \zeta_{P,m,i_1,i_2,i_3}^{\kappa}(k)$$

and

$$[\xi_{l,i_1,i_2,i_3}^{\kappa}(k)]_m = \xi_{l,m,i_1,i_2,i_3}^{\kappa}(k).$$

Evidently, $\mathbf{c}(P,n) = [\mathbf{c}_0^{(P)}(n)^T, \mathbf{c}_1^{(1)}(n)^T, \dots, \mathbf{c}_1^{(P)}(n)^T]^T$ where $[\mathbf{c}_i^{(l)}(n)]_m = c_i^{(l)}(2^lm-n)$ for $i = 0, 1$. Fig. 4 shows a multiresolution analysis ($P = 5$) of a fading coefficient for a time-varying multipath event (500 samples, 41.2- μ sec sampling period, 100 km/h). The representation of the channel is shown at increasing resolutions. Observe that (26) is valid with equality because of the perfect reconstruction property of the dyadic filter bank. We will determine which components of the expansion (26) can be neglected (i.e., zeroed) without compromising the parsimony of the representation.

V. VALIDATION OF THE DWT CHANNEL

Statistical characteristics of the fading channel are typically available from experimental measurements in the form of the scattering function [21]. Assuming the channel to be WSSUS⁴ [1], we can tune our channel representation: in other words, second-order statistics will provide general guidelines on how to select the low-resolution coefficients. Low-resolution coefficients are important for a global characterization of the fading process. It is however important to point out that retaining only the low-resolution coefficients will not give us the kind of “parsimony” that we expect from a wavelet-based representation. To achieve this goal, a few high-resolution coefficients (in addition to the coefficients necessary for a global representation of the process) empirically selected will have to be maintained.

³The notation $[\mathbf{v}]_k$ is used for the k th element of vector \mathbf{v} .

⁴The WSSUS assumption implies $E\{h_{k_1}^{\kappa_1}(t_1, \tau_1)h_{k_2}^{\kappa_2}(t_2, \tau_2)\} = S_{k_1, \kappa_1, k_2, \kappa_2}(\tau_1, t_2 - t_1)\delta(\tau_2 - \tau_1)$, and the expectation is over the channel ensemble. The scattering function of the multipath channel is related to $S_{k_1, \kappa_1, k_2, \kappa_2}(\tau, t)$ by the FT, first with respect to τ , and then with respect to t .

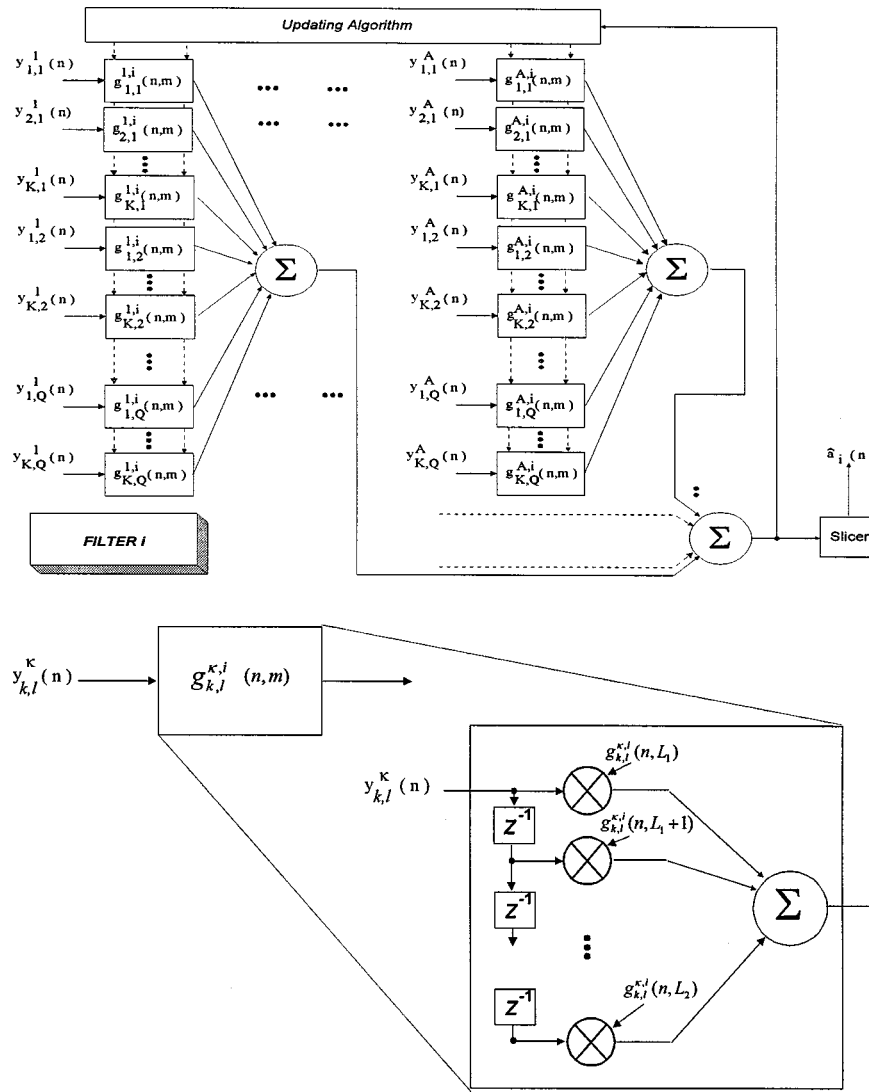


Fig. 4. The (time-varying) filter relative to the i th user.

Having assumed the model (14), the knowledge of the second-order statistics of the channel variations is obtained from the knowledge of

$$E \left\{ f_{k_1, t_1}^{\kappa_1^*}(t_1) f_{k_2, t_2}^{\kappa_2}(t_2) \right\}$$

which is then mapped to the knowledge of the discrete-time autocorrelation function of the channel

$$E \left\{ h_{\mathbf{i}}^{\kappa}(n, k_1) * h_{\mathbf{i}'}^{\kappa'}(n + l, k_2) \right\} = R_h(l, k_1, k_2, \mathbf{i}, \kappa, \mathbf{i}', \kappa')$$

with $\mathbf{i}' = [i'_1, i'_2, i'_3]$, $\mathbf{i} = [i_1, i_2, i_3]$.⁵ Using (26), we have

$$R_h(l, k_1, k_2, \mathbf{i}, \kappa, \mathbf{i}', \kappa') = \mathbf{c}(P, n)^T E \left\{ \mathbf{w}_{\mathbf{i}}^{\kappa}(P, k_1) * \mathbf{w}_{\mathbf{i}'}^{\kappa'}(P, k_2)^T \right\} \mathbf{c}(P, n + l). \quad (28)$$

Observe that due to the orthonormality of the DWT, defining $\mathbf{h}_{\mathbf{i}}^{\kappa}(k)$ as the vector with n th element

$$[\mathbf{h}_{\mathbf{i}}^{\kappa}(k)]_n = h_{\mathbf{i}}^{\kappa}(n, k)$$

⁵In fact, $R_h(l, k_1, k_2, \mathbf{i}, \kappa, \mathbf{i}', \kappa')$ can be computed from the knowledge of $\mathcal{S}_{k_1, \kappa_1, k_2, \kappa_2}(\tau_1, t_2 - t_1)$ and the spreading codes of each user.

we also have

$$E \left\{ \mathbf{w}_{\mathbf{i}}^{\kappa}(P, k_1) * \mathbf{w}_{\mathbf{i}'}^{\kappa'}(P, k_2)^T \right\} = E \left\{ \mathbf{h}_{\mathbf{i}}^{\kappa}(k_1) * \mathbf{h}_{\mathbf{i}'}^{\kappa'}(k_2)^T \right\}$$

which is a matrix constructed from $R_h(l, k_1, k_2, \mathbf{i}, \kappa, \mathbf{i}', \kappa')$. We can validate our model (26) using (28). In other words, we can determine which components of the expansion (26) can be neglected (i.e., zeroed) without compromising the parsimony of the wavelet-based representation. Define $\mathbf{w}_{\mathbf{i}}^{\kappa}(P, k)_{\mathcal{M}}$ as the vector obtained zeroing the last $\sum_{m=1}^{\mathcal{M}} N/2^m$ elements of $\mathbf{w}_{\mathbf{i}}^{\kappa}(P, k)$ and $\mathbf{c}(P, n)_{\mathcal{M}}$ as the vector obtained zeroing the last $\sum_{m=1}^{\mathcal{M}} N/2^m$ elements of $\mathbf{c}(P, n)$. A possible indication of the parsimony in the representation (26) retaining only $N/2^{\mathcal{M}}$ DWT coefficients, $\mathcal{M} = 0, 1, 2, \dots, P$, is

$$\gamma(P, \mathcal{M}) = \sum_{\mathbf{i}, \mathbf{i}'} \sum_{\kappa, \kappa'} \sum_{k_1, k_2} \left\| \mathbf{r}_{\mathbf{i}, \mathbf{i}'}^{\kappa, \kappa'}(k_1, k_2) - \mathbf{v}_{\mathbf{i}, \mathbf{i}'}^{\kappa, \kappa'}(k_1, k_2)_{\mathcal{M}} \right\|^2$$

where

$$\begin{aligned} & \left[\mathbf{v}_{\mathbf{i}, \mathbf{i}'}^{\kappa, \kappa'}(k_1, k_2)_{\mathcal{M}} \right]_l \\ &= \frac{1}{N} \sum_{n=0}^{N-1} \mathbf{c}(P, n)_{\mathcal{M}}^T E \left\{ \mathbf{h}_{\mathbf{i}}^{\kappa}(k_1) * \mathbf{h}_{\mathbf{i}'}^{\kappa'}(k_2)^T \right\} \mathbf{c}(P, n + l)_{\mathcal{M}} \end{aligned}$$

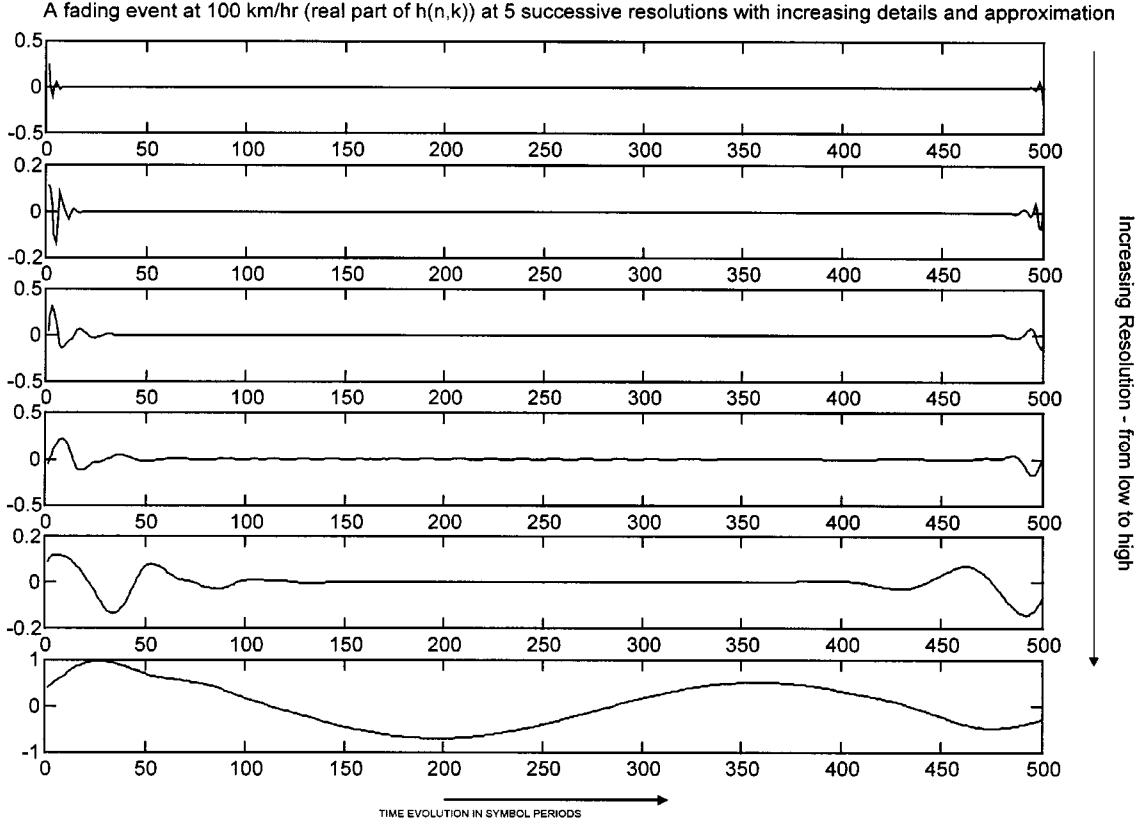


Fig. 5. Multiresolution wavelet-based representation of a fading event (real part of the coefficient for a 500 symbol-spaced samples snapshot) for a time-varying multipath channel representing a mobile transmitter traveling at 100 km/h. The maximum resolution depth is $P = 5$ and the mother wavelet used is generated from a Daubechies filter of order 6.

and $[\mathbf{r}_{\mathbf{i}, \mathbf{i}'}^{\kappa, \kappa'}(k_1, k_2)]_l = R_h(l, k_1, k_2, \mathbf{i}, \kappa, \mathbf{i}', \kappa')$. Once a particular \mathcal{M} has been selected, we can write

$$h_{\mathbf{i}}^{\kappa}(n, k) \simeq \bar{\mathbf{c}}(n)^T \bar{\mathbf{w}}_{\mathbf{i}}^{\kappa}(k) \quad (29)$$

where⁶ $\bar{\mathbf{c}}(n) = \mathbf{I}_{[\mathcal{N}, \bar{\mathcal{N}}]} \mathbf{c}(P, n)$, $\bar{\mathbf{w}}_{\mathbf{i}}^{\kappa}(k) = \mathbf{I}_{[\mathcal{N}, \bar{\mathcal{N}}]} \mathbf{w}_{\mathbf{i}}^{\kappa}(P, k)$ with $\mathcal{N} = N2^{-\mathcal{M}}$, $\bar{\mathcal{N}} = N - \mathcal{N} = N \sum_{m=1}^{\mathcal{M}} 2^{-m}$. Fig. 5 shows a multiresolution wavelet-based decomposition for a 100-km/h fading channel. Fig. 6 shows experiments for the time-varying multipath DWT decomposition of a 500-samples (symbol spaced) snapshot. From top to bottom of the figure: the magnitude of a generic Rayleigh fading tap, DWT ($P = 5$) for the real part of the tap variations, dynamics of the real part and reconstructed dynamics using 16 wavelet coefficients. In Fig. 7, we show the approximation error for different resolution depths P and for different values of \mathcal{M} for $N = 512$. The approximation error (shown in decibels in Fig. 3) is defined as

$$\text{MSE}_h = E \left\{ \left| h_{\mathbf{i}}^{\kappa}(n, k) - \bar{\mathbf{c}}(n)^T \bar{\mathbf{w}}_{\mathbf{i}}^{\kappa}(k) \right|^2 \right\}$$

where $\bar{\mathbf{c}}(n)$ and $\bar{\mathbf{w}}_{\mathbf{i}}^{\kappa}(k)$ contain, for any indicated P , only $512/2^{-\mathcal{M}}$ components.

⁶The notation \mathbf{I}_A identifies the $A \times A$ identity matrix, while the notation $\mathbf{I}_{[A, B]}$ identifies the $A \times (A+B)$ matrix whose first A columns are the columns of \mathbf{I}_A and the last B columns have elements equal to zero.

A. Interpretations

The method we have outlined can be interpreted as a subspace selection procedure [24]. In fact, the DWT of the N -long vector $\mathbf{h}_{\mathbf{i}}^{\kappa}(k)$ representing the dynamics of the channel at lag k can be expressed as

$$\mathbf{h}_{\mathbf{i}}^{\kappa}(k) = \mathbf{W} \mathbf{w}_{\mathbf{i}}^{\kappa}(P, k) \quad (30)$$

where \mathbf{W} is an $N \times N$ orthonormal linear transformation expressing the operation of the wavelet transform. Consider $\bar{\mathbf{W}} = [\mathbf{W}_1, \dots, \mathbf{W}_{\mathcal{N}}]^T$, the $N \times \mathcal{N}$ matrix formed by the first $\mathcal{N} = N2^{-\mathcal{M}}$ columns of \mathbf{W} corresponding to the *shrinkage* (that is the zeroing) that yields tolerably small values of the metric $\gamma(P, \mathcal{N})$. Applying the transformation

$$\theta_{\mathbf{i}}^{\kappa}(k) = \bar{\mathbf{W}}^H \mathbf{h}_{\mathbf{i}}^{\kappa}(k) \quad (31)$$

we essentially define a “subspace parameter” $\theta_{\mathbf{i}}^{\kappa}(k)$. The \mathcal{N} orthonormal columns of $\bar{\mathbf{W}}$ span an \mathcal{N} -dimensional subspace defined $\mathcal{W}_{\mathcal{N}}$ such that $\mathcal{W}_{\mathcal{N}} \subseteq \mathcal{C}^N$ (the space of any complex vector of length N). Observe that when the transformation $\bar{\mathbf{W}}$ is selected with $\mathcal{N} < N$, any estimate (or representation) of $\theta_{\mathbf{i}}^{\kappa}(k)$ is insensitive to disturbance components of $\mathbf{h}_{\mathbf{i}}^{\kappa}(k)$ for $m = \mathcal{N} + 1, \mathcal{N} + 2, \dots, N$, and the resulting estimator (or representation) has a smaller variance than the full space estimator. Also, any traditional adaptive scheme for equalization (or channel tracking) designed to follow the variations of $h_{i_1, i_2, i_3}^{\kappa}(n, k)$ attempts a full-space estimation of the channel. In other words, traditional schemes will generate point-by-point estimates spanning \mathcal{C}^N . The proposed channel representation

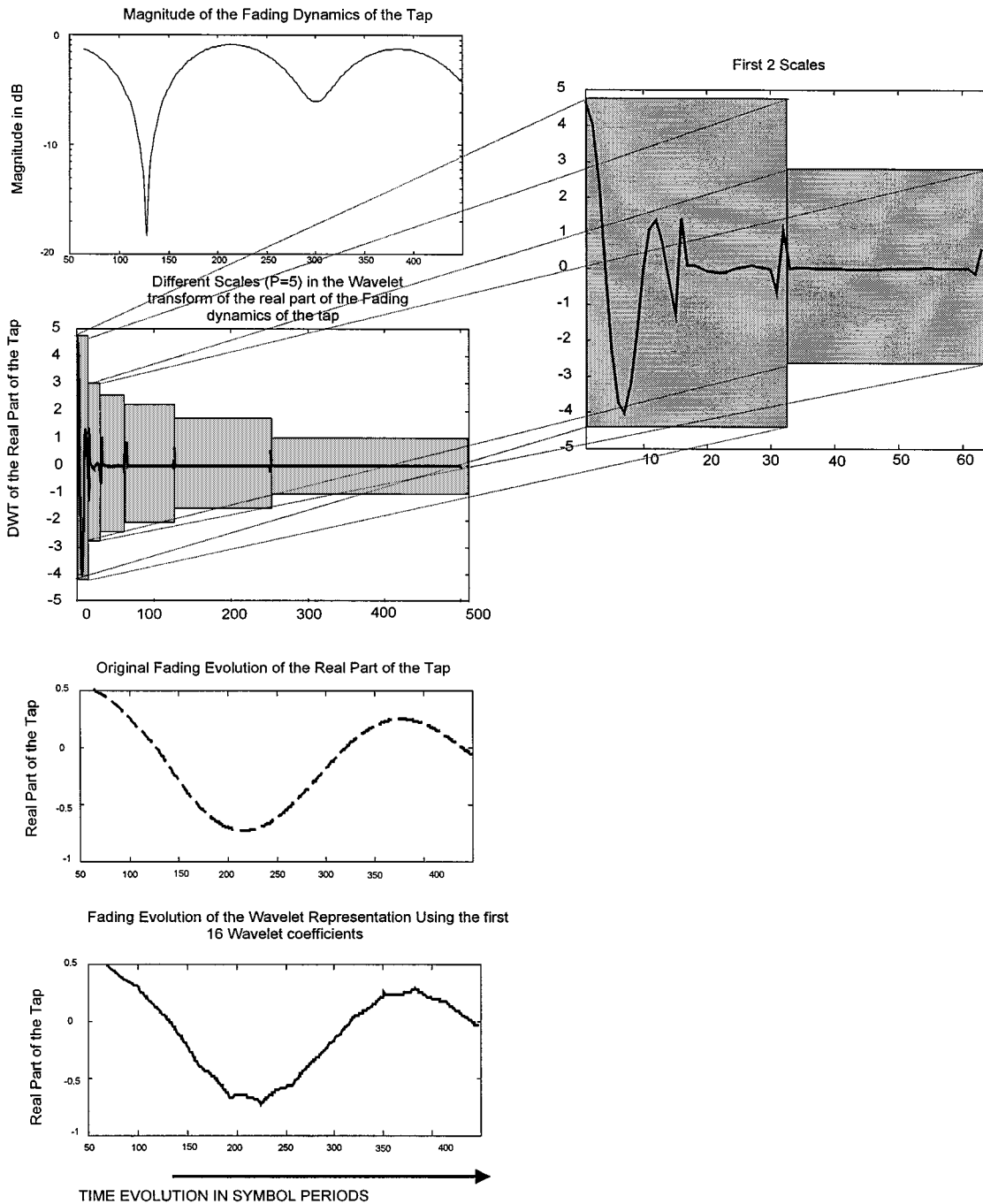


Fig. 6. An example of time-varying multipath DWT decomposition for a 500-sample (symbol spaced) snapshot. From top to bottom: the magnitude of a generic Rayleigh fading tap, DWT ($P = 5$) for the real part of the tap variations, dynamics of the real part and reconstructed dynamics using only 16 wavelet coefficients.

method when incorporated in practical detectors will achieve a decreased variance of the channel estimate error. It is however important to emphasize that this advantage is obtained at the expense of estimation bias, because in practice

$$\mathbf{h}_i^\kappa(k) = \bar{\mathbf{W}}\theta_i^\kappa(k) = \mathbf{P}_W\mathbf{h}_i^\kappa(k) \quad (32)$$

with $\mathbf{P}_W = \bar{\mathbf{W}}\bar{\mathbf{W}}^H$ holds only approximately true, and while the variance increases with the dimensions of the subspace (that is \mathcal{N}), the bias decreases [24]. Evidently, the goal of selecting a transformation $\bar{\mathbf{W}}$ is to optimize the tradeoff between bias, variance, and computational load.

VI. DETECTORS

Once we have achieved a parsimonious representation of the form (29), we can write (16) as

$$\begin{aligned} y_{i,l}^\kappa(n) &= \sum_{k=1}^K \sum_m \bar{\mathbf{c}}(n)^T \bar{\mathbf{w}}_{i,k,l}^\kappa(m) a_k(n-m) + \eta_{i,l}^\kappa(n) \\ &= \mathbf{a}(n)^T \mathbf{C}(n) \mathbf{w}_{i,l}^\kappa + \eta_{i,l}^\kappa(n) \\ &= \tilde{\mathbf{a}}(n)^T \mathbf{w}_{i,l}^\kappa + \eta_{i,l}^\kappa(n), \\ i &= 1, 2, \dots, K; \kappa = 1, 2, \dots, A; l = 1, 2, \dots, Q \end{aligned} \quad (33)$$

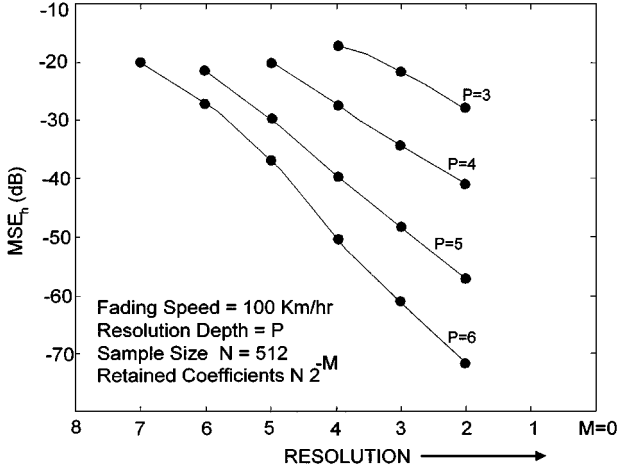


Fig. 7. Mean squared error (MSE) (average over 100 experiments) of the multiresolution wavelet-based representation of a fading process (real part of the coefficient for a $N = 512$ symbol-spaced samples snapshot) for a time-varying multipath channel representing a mobile transmitter traveling at 100 km/h. The maximum resolution depth is P , and the mother wavelet used is generated from a Daubechies filter of order 6. The MSE is plotted versus M where $N/2^M$ is the number of wavelet coefficients maintained in the representation of the 512-point sample evolution.

where $\tilde{\mathbf{a}}(n) = \mathbf{C}(n)^T \mathbf{a}(n)$, and the organization of the filterbank coefficients into $\mathbf{C}(n)$ and the wavelet coefficients into $\mathbf{w}_{i,l}^{\kappa}$ is evident from the context. We can compact in matrix notation (33) organizing the samples $y_{i,l}^{\kappa}(n)$ for $n = 0, 1, 2, \dots, M-1$, $i = 1, 2, \dots, K$, $\kappa = 1, 2, \dots, A$, $l = 1, 2, \dots, Q$ in a vector \mathbf{y}_M to obtain the familiar model

$$\mathbf{y}_M = \mathbf{A}_M(\mathbf{a})\mathbf{w} + \mathbf{n} \quad (34)$$

where \mathbf{w} is a vector that contains the wavelets coefficients and $\mathbf{A}_M(\mathbf{a})$ depends uniquely on the MK transmitted symbols $\mathbf{a} = [a_1(0), \dots, a_K(M-1)]^T$ and the coefficients of the filterbank (ultimately the selected orthonormal basis). Using a generalized likelihood [28] argument, we can obtain the (blind) ML rule [15]

$$\hat{\mathbf{a}} = \arg \min_{\alpha} \mathbf{y}_M^H \mathbf{Q}_{\alpha} \mathbf{y}_M \quad (35)$$

$$= \arg \max_{\alpha} \mathbf{y}_M^H \mathbf{P}_{\alpha} \mathbf{y}_M \quad (36)$$

where α is the hypothesized sequence, $\mathbf{Q}_{\alpha} = \mathbf{I} - \mathbf{P}_{\alpha}$, and

$$\mathbf{P}_{\alpha} = \mathbf{A}_M(\alpha) [\mathbf{A}_M(\alpha)^H \mathbf{R}_n^{-1} \mathbf{A}_M(\alpha)]^{-1} \mathbf{A}_M(\alpha)^H \mathbf{R}_n^{-1}$$

is the novel separating kernel with $\mathbf{R}_n = E\{\mathbf{nn}^H\}$. The generalized ML rule in (36) presents significant complexity, if quite attractive conceptually. Indeed, it is rarely practical. A more feasible approach is to design a time-variant minimum average squared-error filter that attempts restoration of the desired user.

A. Time-Variant Filter

A possible solution to detection is to implement a time-variant minimum average square-error (MASE) filter for the k th user indicated at time n as $g_{i,l}^{\kappa,k}(n, m)$, $m = L_1, L_1 + 1, \dots, L_2$, $i =$

$1, 2, \dots, K$, $l = 1, 2, \dots, Q$, $\kappa = 1, 2, \dots, A$, as indicated in Fig. 4. Denote $\hat{a}_k(n)$ as the output of the filter for the detection of the n th symbol of the k th user

$$\sum_{i=1}^K \sum_{l=1}^Q \sum_{\kappa=1}^A \sum_{m=L_1}^{L_2} g_{i,l}^{\kappa,k}(n, m) y_{i,l}^{\kappa}(n - m) = \hat{a}_k(n). \quad (37)$$

The filter coefficients can be obtained from the minimization of the averaged squared error

$$\left\langle \left| \sum_{i=1}^K \sum_{l=1}^Q \sum_{\kappa=1}^A \sum_{m=L_1}^{L_2} g_{i,l}^{\kappa,k}(n, m) y_{i,l}^{\kappa}(n - m) - a_k(n) \right|^2 \right\rangle_N \quad (38)$$

where we have used the notation $\langle x_n \rangle_N = (1/N) \sum_{n=1}^N x_n$ for an N -sample time average. The orthogonality principle dictates that

$$\left\langle \left(\sum_{i=1}^K \sum_{l=1}^Q \sum_{\kappa=1}^A \sum_{m_1=L_1}^{L_2} g_{i,l}^{\kappa_1,k}(n, m) y_{i,l}^{\kappa_1}(n - m_1) - a_k(n) \right) y_{p,q}^{\kappa_2}(n - m_2) \right\rangle_N = 0 \quad (39)$$

for $\kappa_2 = 1, \dots, A$, $p = 1, \dots, K$, $q = 1, \dots, Q$, $m_2 = L_1, \dots, L_2$.

Since we have established that a reasonably accurate representation of the fading channel variations is given by (29), it is also intuitively clear that the optimum time-variant filter can be expressed as

$$g_{i_1, i_2}^{\kappa, k}(n, m) \simeq \bar{\mathbf{c}}(n)^T \bar{\mathbf{w}}_{[g]_{i_1, i_2}}^{\kappa, k}(m).$$

A more detailed explanation of this last statement is in the Appendix. Renaming more conveniently the components of $\bar{\mathbf{c}}(n)$ and $\bar{\mathbf{w}}_{[g]_{i_1, i_2}}^{\kappa}(k)$ as

$$\bar{\mathbf{c}}(n) = [c_1(n), c_2(n), \dots, c_N(n)]^T$$

$$\bar{\mathbf{w}}_{[g]_{i_1, i_2}}^{\kappa}(k) = [\bar{w}_{[g]_{i_1, i_2}}^{\kappa}(k)_1, \bar{w}_{[g]_{i_1, i_2}}^{\kappa}(k)_2, \dots, \bar{w}_{[g]_{i_1, i_2}}^{\kappa}(k)_N]^T$$

we can use the following expression:

$$g_{i_1, i_2}^{\kappa, k}(n, m) \simeq \bar{\mathbf{c}}(n)^T \bar{\mathbf{w}}_{[g]_{i_1, i_2}}^{\kappa, k}(m) = \sum_{p=1}^N \bar{w}_{[g]_{i_1, i_2}}^{\kappa, k}(m)_p c_p(n)$$

and obtain

$$\left\langle \left| \sum_{i=1}^K \sum_{l=1}^Q \sum_{\kappa=1}^A \sum_{m=L_1}^{L_2} g_{i,l}^{\kappa,k}(n, m) y_{i,l}^{\kappa}(n - m) - a_k(n) \right|^2 \right\rangle_N \\ = \left\langle \left| \sum_{i=1}^K \sum_{l=1}^Q \sum_{\kappa=1}^A \sum_{m=L_1}^{L_2} \sum_{p=1}^N \bar{w}_{[g]_{i,l}}^{\kappa,k}(m)_p c_p(n) y_{i,l}^{\kappa}(n - m) - a_k(n) \right|^2 \right\rangle_N.$$

If we denote $\tilde{y}_{i,l,p}^{\kappa}(n, m) = c_p(n)y_{i,l}^{\kappa}(n-m)$, the orthogonality principle can be expressed as

$$\left\langle \left(\sum_{i_1=1}^K \sum_{l_1=1}^Q \sum_{\kappa_1=1}^A \sum_{m_1=L_1}^{L_2} \sum_{p_1=1}^{\mathcal{N}} \bar{w}_{[g]_{i_1, l_1}}^{\kappa_1, k} (m_1)_{p_1} \right. \right. \\ \left. \left. \times \tilde{y}_{i_1, l_1, p_1}^{\kappa_1} (n, m_1) - a_k(n) \right) \tilde{y}_{i_2, l_2, p_2}^{\kappa_2} (n, m_2) \right\rangle_N = 0 \quad (40)$$

for $\kappa_2 = 1, \dots, A$, $i_2 = 1, \dots, K$, $l_2 = 1, \dots, Q$, $m_2 = L_1, \dots, L_2$, $p_2 = 1, \dots, \mathcal{N}$. It is easily shown that the solution to this estimation problem is

$$\mathbf{w}_{[g]_k} = \mathbf{R}^{-1} \mathbf{d}_k \quad (41)$$

where

$$\mathbf{w}_{[g]_k} = \left[\mathbf{w}_{[g]_k}^1, \mathbf{w}_{[g]_k}^2, \dots, \mathbf{w}_{[g]_k}^A \right]^T \\ \mathbf{w}_{[g]_k}^{\kappa} = \left[\mathbf{w}_{[g]_{1,1}}^{\kappa, k}, \dots, \mathbf{w}_{[g]_{K,1}}^{\kappa, k}, \dots, \mathbf{w}_{[g]_{K,Q}}^{\kappa, k} \right]^T \\ \mathbf{w}_{[g]_{j,t}}^{\kappa, k} = \left[\bar{w}_{[g]_{j,t}}^{\kappa, k} (L_1)_1, \dots, \bar{w}_{[g]_{j,t}}^{\kappa, k} (L_2)_1, \dots, \bar{w}_{[g]_{j,t}}^{\kappa, k} (L_2)_{\mathcal{N}} \right]^T \\ \mathbf{R} = \langle \tilde{\mathbf{y}}_c^*(n) \tilde{\mathbf{y}}_c(n) \rangle_N \quad (42)$$

$$\mathbf{d}_k = \langle \tilde{\mathbf{y}}_c^*(n) a_k(n) \rangle_N \quad (43)$$

with

$$\tilde{\mathbf{y}}_c(n) = \left[\tilde{\mathbf{y}}_c^1(n)^T, \tilde{\mathbf{y}}_c^2(n)^T, \dots, \tilde{\mathbf{y}}_c^A(n)^T \right]^T \\ \tilde{\mathbf{y}}_c^{\kappa}(n) = \left[\mathbf{y}_{c_{1,1}}^{\kappa}(n)^T, \dots, \mathbf{y}_{c_{K,2}}^{\kappa}(n)^T, \dots, \mathbf{y}_{c_{K,Q}}^{\kappa}(n)^T \right]^T \\ \mathbf{y}_{c_{i,t}}^{\kappa}(n) = \left[\tilde{y}_{i,l_1}^{\kappa}(n, L_1), \tilde{y}_{i,l_1}^{\kappa}(n, L_2), \dots, \tilde{y}_{i,l_{\mathcal{N}}}^{\kappa}(n, L_2) \right]^T. \quad (44)$$

Typical approaches to achieve real-time implementation are gradient-based methods and recursive least squares (RLS)-based methods. The well-known recursion in both cases is

$$\mathbf{w}_{[g]_k}(n+1) = \mathbf{w}_{[g]_k}(n) + \mathbf{P}_n \left[\tilde{\mathbf{y}}_c(n), \mathbf{w}_{[g]_k}(n) \right] \quad (45)$$

where

$$\mathbf{P}_n \left[\tilde{\mathbf{y}}_c(n), \mathbf{w}_{[g]_k}(n) \right] = \mu \left(a_k(n) - \tilde{\mathbf{y}}_c(n)^T \mathbf{w}_{[g]_k}(n) \right) \tilde{\mathbf{y}}_c^*(n)$$

if the algorithm of choice is the least mean square (LMS) and μ is a step-size parameter that controls the rate of adjustment. Using an RLS approach, we have $\mathbf{P}_n \left[\tilde{\mathbf{y}}_c(n), \mathbf{w}_{[g]_k}(n) \right] = \lambda \mathbf{K}_n^* \epsilon_n$ where $\epsilon_n = a_k(n) - \tilde{\mathbf{y}}_c(n)^T \mathbf{w}_{[g]_k}(n)$, $\mathbf{K}_n = (\mathbf{P}_{n-1} \mathbf{a}_n) / (\lambda + \tilde{\mathbf{y}}_c(n)^H \mathbf{P}_{n-1} \tilde{\mathbf{y}}_c(n))$ and $\mathbf{P}_n = \lambda^{-1} (\mathbf{P}_{n-1} - \tilde{\mathbf{y}}_c(n)^H \mathbf{P}_{n-1} \mathbf{K}_n)$. λ is a forgetting factor that can be set approximately equal to one because, in reality, the wavelet coefficients are time-invariant and need only to be identified, not tracked.

Remark 1: It is important to observe that the true vector of wavelet coefficients is time invariant, so the task of the adaptive algorithm in the proposed approach is to converge to the channel parameters as opposed to *track* them. This makes the LMS algorithm perfectly adequate for the task. If the WBD retains $N2^{-M}$ wavelet coefficients, then the complexity of the

proposed approach is $\mathcal{O}[LKA2^{-M}]$ for an L long filter, K users, and A antennas. In the traditional minimum MSE (MMSE) approach, one is forced to use an RLS approach because tracking directly the taps of the filter using a gradient approach is ineffective in fast fading. Evidently, one ends up with a complexity $\mathcal{O}[(LKA)^2]$, which in most cases is much higher than the complexity presented by the WBD multiscale filter approach for the same length of the filter, number of antennas, and number of users. This advantage in fast fading environments is extremely valuable and in fact results in significant performance advantages.

Remark 2: One of the reviewers (reviewer B) suggested an interesting interpretation of the expression in (41). There is an apparent similarity between (41) and the MMSE linear multiuser detector of [13]. In particular, the two detectors converge asymptotically to the same detector in the case of time-invariant channels. It is then appropriate to state that the detector described by (41) in a rapidly varying environment is a practical approximation of the instantaneous exact Wiener solution. The instantaneous Wiener filter cannot be implemented in a time-varying environment using average sample-statistics estimators because the processes involved are nonstationary. This is exactly the reason why the detector (41) outperforms the traditional multiuser MMSE detector (see Section VII), which uses sample-statistics averages for the estimation of second-order statistics.

VII. PERFORMANCE ANALYSIS

Since an analytical approach to the performance of the outlined detector is beyond the scope and the length of this paper, we present the results of a simulation analysis. Consider a mobile radio system when the uplink applies DS/CDMA with a gross bit rate equal to 48.5 kbit/s. The users' codes are known at the receiver as the base station has allocated one code for each user. We use Gold codes of 15 chips, 7 equipower users, and $Q = 2$ (two-path Rayleigh fading channel) in each channel impulse response between each user and each antenna array element. The antenna is a three-element uniform linear array with $3/4$ of a wavelength spacing (this spacing guarantees uncorrelated scattering at the different antennas). The impulse responses of the multipath channels are generated so that the delays are constrained to be an integer number of chip periods according to Table I. Users modulate data using quadrature phase-shift keying (QPSK). A synchronization unit is assumed to estimate the delays exactly. We assume the first user to be the reference user. Signal-to-noise ratio (SNR) in the figures is equal to E_b^s/N_0 . A training sequence of 14 symbols is transmitted every 256 symbols, to train the time-variant filter.

The slots are generated of dyadic length and $C_0(z)C_1(z)$ are Daubechies filters of order 3. We assume [12] that

$$R_n(l, k_1, k_2, \mathbf{i}, \kappa, \mathbf{i}', \kappa') \\ = \begin{cases} \sigma_k^2 J_0(2\pi l f_D T/R), & \text{for } k_1 = k_2 = k \text{ and } \mathbf{i} = \mathbf{i}' \\ 0, & \text{elsewhere} \end{cases}$$

where $J_0(x)$ is the Bessel function of order zero, f_D is Doppler spread that depends on the velocity of the mobile transmitter, σ_k^2 is the variance of the fading process. The Doppler frequency

TABLE I
CHANNEL PROPAGATION ENVIRONMENTS FOR PERFORMANCE
EVALUATION RESULTS: DELAY SPREADS OF THE MOBILES

User	$\tau_{k,1}^1, \tau_{k,2}^1$	$\tau_{k,1}^2, \tau_{k,2}^2$	$\tau_{k,1}^3, \tau_{k,2}^3$	Speed
1	$0T_c, 2T_c$	$1T_c, 2T_c$	$1T_c, 4T_c$	100 Km/hr
2	$1T_c, 3T_c$	$0T_c, 2T_c$	$3T_c, 4T_c$	80 Km/hr
3	$0T_c, 4T_c$	$1T_c, 5T_c$	$3T_c, 4T_c$	50 Km/hr
4	$1T_c, 2T_c$	$2T_c, 3T_c$	$3T_c, 4T_c$	10 Km/hr
5	$1T_c, 1T_c$	$2T_c, 4T_c$	$3T_c, 4T_c$	20 Km/hr
6	$2T_c, 4T_c$	$1T_c, 3T_c$	$3T_c, 4T_c$	80 Km/hr
7	$1T_c, 5T_c$	$2T_c, 3T_c$	$3T_c, 4T_c$	100 Km/hr

describes the second-order statistics of channel variations. Doppler frequency is related through wavelength $\tilde{\lambda}$ to the i th mobile transmitter velocity V_i expressed in km/h. The complex weights are generated as filtered Gaussian processes fully specified by the scattering function. Particularly, each process has a frequency response equal to the square root of the Doppler power density spectrum.⁷ It is then straightforward to verify (using the described validation method) that for speeds of the mobile up to 300 km/h and $P = 4$ or $P = 5$, it is possible to retain only $N/2^M = 32$ or $N/2^M = 16$ wavelet coefficients in $\mathbf{w}_{i_1, i_2, i_3}^{\kappa}(P, k)$ without significant penalty in the matching metric $\gamma(P, \mathcal{M})$. In other words, the excellent ‘‘compacting’’ properties (see [7]) of the wavelet transform are able to compress most of the energy of the time variations of the channel in the low-resolution representation of the fading process, and this makes the approach very attractive in practice. The output of the filter at time step n is $\tilde{\mathbf{y}}_c(n)^T \mathbf{w}_{[g]_k}(n)$, where the vector $\mathbf{w}_{[g]_k}(n)$ is obtained from $\mathbf{w}_{[g]_k}(n-1)$, $\hat{a}_k(n-1)$, $\tilde{\mathbf{y}}_c(n-1)$ as in (45).⁸ The vector $\tilde{\mathbf{y}}_c(n)$ is computed from the baseband samples and the coefficients of the Daubechies filters $c_0(n)$ and $c_1(n)$ at each antenna as detailed in (44). A decision for the n th symbol for the k th user is obtained from a QPSK slicer whose input is the scalar $\tilde{\mathbf{y}}_c(n)^T \mathbf{w}_{[g]_k}(n)$. Bit-error rate (BER) analysis results are shown in Figs. 8 and 9. We compare with the multiuser MMSE detector updated using the QR-RLS (QR-based recursive least squares) algorithm (probably the best method in terms of tracking performance). The MMSE-QR-RLS at every iteration solves the following minimization problem:

$$\min_{\mathbf{g}_k} \left\| \begin{bmatrix} \lambda \mathbf{Y}(n) \\ \tilde{\mathbf{y}}(n+1)^T \end{bmatrix} \mathbf{g}_k - \begin{bmatrix} \lambda \mathbf{a}_k(n) \\ a_k(n+1) \end{bmatrix} \right\|^2 \quad (46)$$

where $\mathbf{Y}(n)$ and $\mathbf{a}(n)$ are recursively defined as

$$\mathbf{Y}(n) = \begin{bmatrix} \lambda \mathbf{Y}(n-1) \\ \tilde{\mathbf{y}}(n)^T \end{bmatrix}, \quad \mathbf{a}_k(n) = \begin{bmatrix} \lambda \mathbf{a}_k(n-1) \\ a_k(n) \end{bmatrix}$$

⁷The Doppler spectrum is approximated by rational filtered processes. The filters are described by their 3-dB bandwidth, which is called the normalized Doppler frequency. The additional assumption is that all channels and complex weights have the same Doppler spectrum.

⁸ $\hat{a}_k(n-1)$ is the decision on the complex QPSK n th symbol, k th user. Evidently, the filter runs in decision-directed mode. While in training, the exact knowledge of the first 14 symbols allow the estimation of $\mathbf{w}_{[g]_k}(n)$ using (41).

with

$$\begin{aligned} \tilde{\mathbf{y}}(n) &= [\tilde{\mathbf{y}}^1(n)^T, \tilde{\mathbf{y}}^2(n)^T, \dots, \tilde{\mathbf{y}}^A(n)^T]^T \\ \tilde{\mathbf{y}}^{\kappa}(n) &= [\mathbf{y}_{1,1}^{\kappa}(n)^T, \dots, \mathbf{y}_{1,Q}^{\kappa}(n)^T, \dots, \mathbf{y}_{K,Q}^{\kappa}(n)^T]^T \\ \mathbf{y}_{i,l}^{\kappa}(n) &= [y_{i,l}^{\kappa}(n-L_1), \dots, y_{i,l}^{\kappa}(n-L_2)]^T \\ \mathbf{g}_k &= [\mathbf{g}_k^{1T}, \mathbf{g}_k^{2T}, \dots, \mathbf{g}_k^{AT}]^T \\ \mathbf{g}_k^{\kappa} &= [\mathbf{g}_{1,1}^{\kappa,kT}, \dots, \mathbf{g}_{K,2}^{\kappa,kT}, \dots, \mathbf{g}_{1,Q}^{\kappa,kT}, \dots, \mathbf{g}_{K,Q}^{\kappa,kT}]^T \\ \mathbf{g}_{j,l}^{\kappa,k} &= [\bar{g}_{j,l}^{\kappa,k}(L_1), \bar{g}_{j,l}^{\kappa,k}(L_1+1), \dots, \bar{g}_{j,l}^{\kappa,k}(L_2)]^T. \end{aligned}$$

The solution obtained by applying a recursive QR decomposition to the data matrix $\mathbf{Y}(n)$ defines the QR-RLS [19] algorithm, which attempts convergence to the MMSE solution for \mathbf{g}_k . We use in the DWT representation of the time-variant filter $P = 4$ and retain $N/2^M = 32$ (for $N = 256$). The BER is relative to the first mobile transmitter. Ideal frame and symbol synchronization is assumed, and the LMS is used to update the wavelet coefficients. A sample size of 10^{k+4} was used to estimate an error probability of 10^{-k} . Fig. 8 shows results for the propagation environment reported in Table I, which evidently represents a fast fading environment, such as those practically found in high-mobility cellular systems. $L = L_2 - L_1 + 1$ is the length of the filter, A is the number of sensors at the receiving antenna array. It is clear that the MMSE approach (dashed curves in Fig. 6) is inadequate. Fig. 9 shows the results of experiments with only the first three users active simultaneously. The speed of the three mobile transmitters is increased up to 400 km/h, the SNR per bit is equal to 32 dB. The DWT-based filter is significantly less sensitive to Doppler spread increases.

A. Hardware Implementation Results

A simpler scenario ($K = 2, A = 2, Q = 2$) was studied using baseband data collected from the DSP receiver section of Base₂, the dual-mode wide-band base station implemented at Watkins-Johnson Company [16]–[18]. A block diagram of the receiver section of the base station was shown in [16]. The wide-band base-station architecture is described in detail in [30]. Fig. 10 outlines the hardware setup. The dispersive channel is created using two hardware fading emulators (NoiseCom MP1600) which model two-ray Rayleigh fading channels. The signal generator simulates transmission of CDMA frames from two different mobiles with the frame format described in the previous section. The DSP modem receives two complex I, Q pairs at the rate of 727.5 kHz after RF conversion and digital quadrature downconversion. The wordlength used is 24 bits and the algorithm has been implemented using simulated fixed-point arithmetic. Automatic gain control is operated on a slot-by-slot basis to exploit full dynamic range of the digital signal processing unit. While perfect synchronization was assumed in the previous simulations, in the hardware experiments, there is an open-loop synchronizer (both PN code and frame synchronization). We use a resolution depth equal to $P = 5$ and $\mathcal{M} = 3, 4, 5$ (that is, we keep 8, 16, 32 wavelet coefficients). The results of extensive BER measurements are

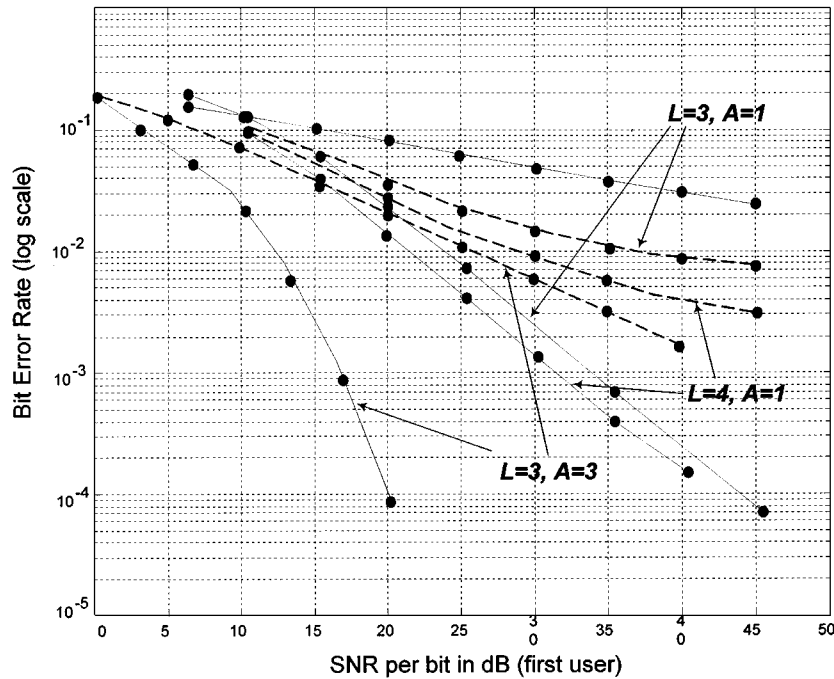


Fig. 8. BER for seven users, 15-length Gold codes in fast frequency-selective fading channels. For propagation parameters, see Table I. Solid curves are for the time-varying separating filter based on the DWT representation. Dashed curves are for the MMSE time-invariant filter based on the traditional adaptive QR-RLS scheme.

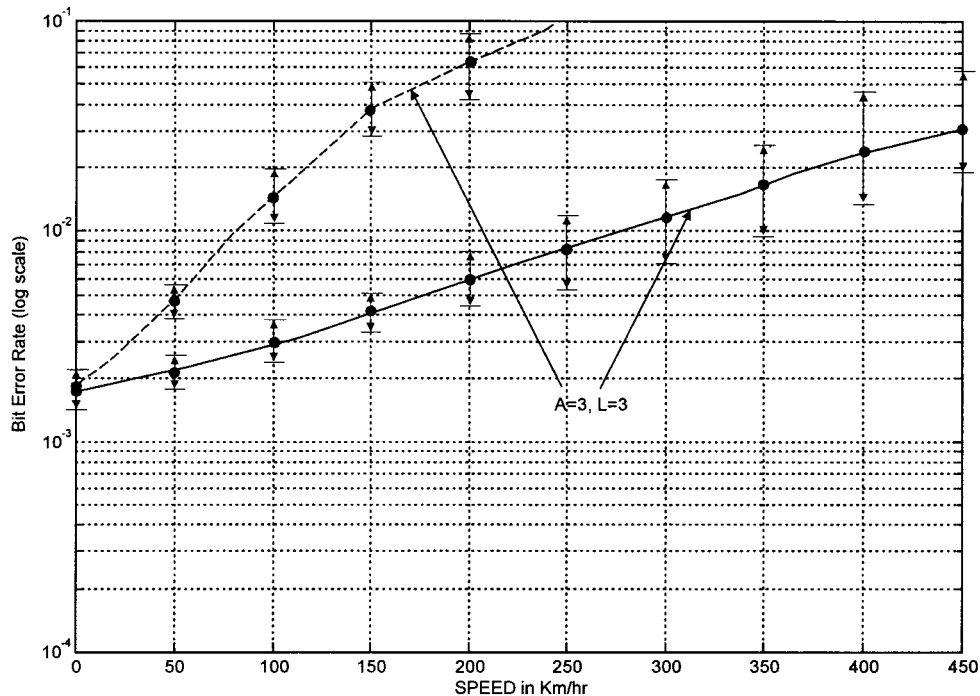


Fig. 9. BER for three users, 15-length Gold codes in fast frequency-selective fading channels with increasing speed of user 1, 2, 3. For propagation parameters, see Table I (first three users). Solid curves are for the time-variant separating filter based on the DWT representation. Dashed curves are for the MMSE time-invariant filter based on the traditional adaptive QR-RLS scheme. The 90% confidence intervals for the measured BER are shown.

summarized in Fig. 11. The propagation environment is described in Table I, considering only the first two users and first two antennas. The complexity of the algorithm is for $L = 4$, $A = 2$, $K = 2$ equivalent to 78 MIPS (millions of instructions per second), which is well within current processing capability of most DSP processors today on the market.

VIII. CONCLUSION

A new multipath fading channel representation based on wavelets allowed a new formulation of the CDMA detection problem in frequency-selective rapidly fading channels. The channel time variations were decomposed using optimal

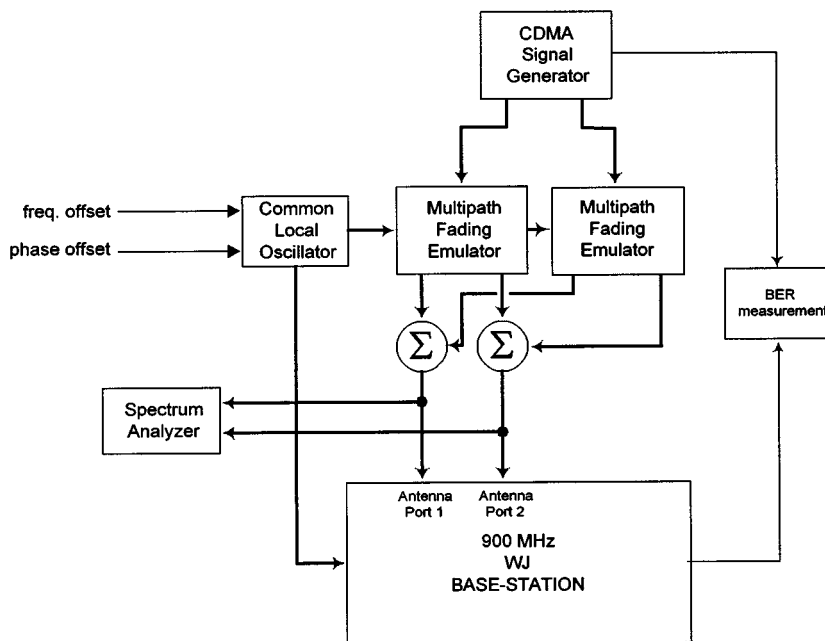


Fig. 10. Hardware test setup for lab experiments.

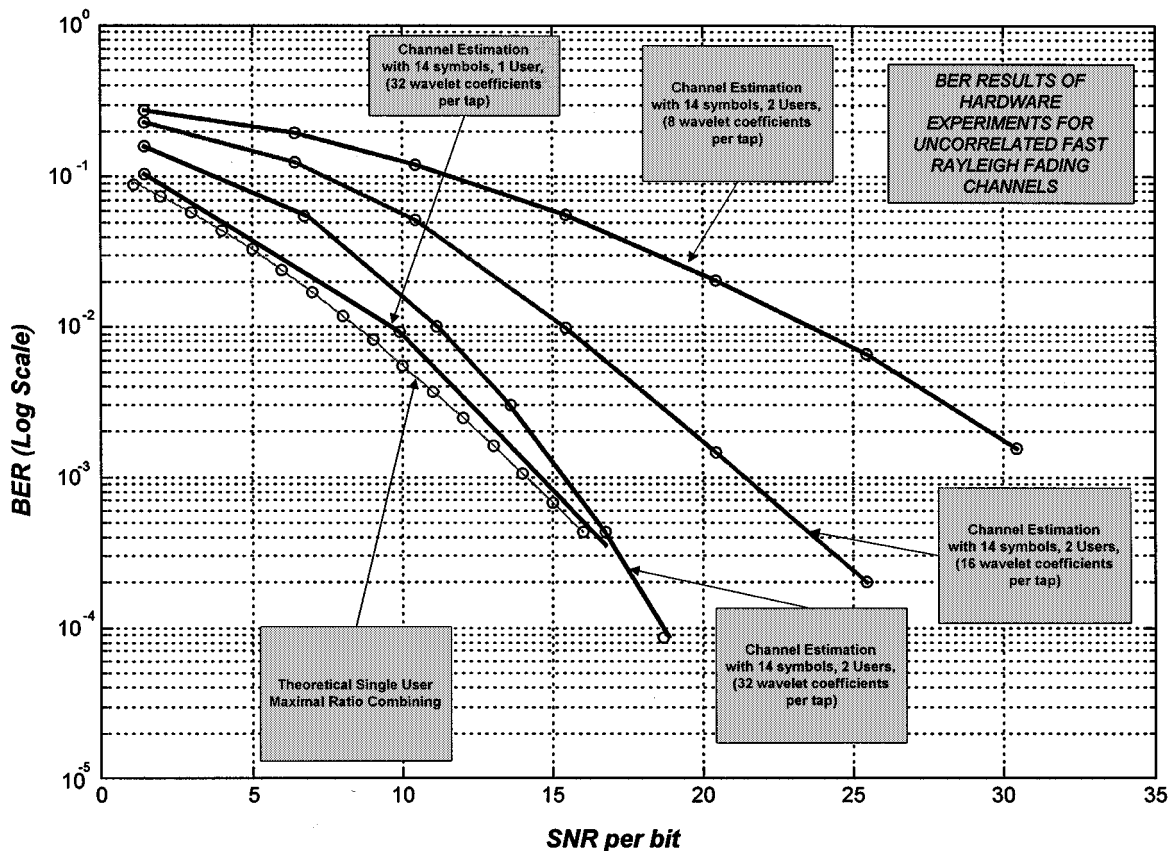


Fig. 11. BER for hardware experiments with one or two users, two antennas, 15-length Gold codes in fast frequency-selective fading channels. The length of the filter is $L = 4$. For propagation parameters, see Table I (first two users, first two antennas).

unconditional bases such as orthonormal wavelet bases. The use of these expansions is well motivated by the excellent time-frequency localization properties of the wavelet functions. Particularly, the time-localization allows a “parsimonious” (that is, economical while still accurate) representation of

the channel dynamics over the time of observation. This cannot possibly be achieved using traditional time-only or frequency-only processing techniques. Using the new model, we have formulated the generalized likelihood detection statistics which, however, present an unmanageable complexity. As a

practical solution, we focused on a multiscale time-variant adaptive filter characterized by the same dynamical features exhibited by the channel, and we proved the approach extremely effective with respect to the traditional MMSE multiuser receiver. Simulation results and hardware experiments have been shown to demonstrate that the approach can be more effective than traditional algorithms in time-varying channels characterized by large Doppler spread.

APPENDIX

In this appendix, we give a justification to the statement we made in Section V-A.

If the time variations of the multipath responses are well represented by an expansion of the form

$$h_{i_1, i_2, i_3}^{\kappa}(n, m) = \mathbf{c}(P, n)^T \mathbf{w}_{i_1, i_2, i_3}^{\kappa}(P, m) \quad (47)$$

where $\mathbf{c}(P, n)^T$ are coefficients of the discrete-time basis and $\mathbf{w}_{i_1, i_2, i_3}^{\kappa}(P, m)$ are coefficients of the expansion, then it is very reasonable to expect that the time-varying filter that minimizes the MSE between $a_k(n)$ and $\sum_{i=1}^K \sum_{l=1}^Q \sum_{\kappa=1}^A \sum_{m=L_1}^{L_2} g_{i,l}^{\kappa,k}(n, m) y_{i,l}^{\kappa}(n - m)$ also can be represented as

$$g_{i_1, i_2}^{\kappa,k}(n, m) \simeq \mathbf{c}(n)^T \mathbf{w}_{[\mathbf{g}]_{i_1, i_2}}^{\kappa,k}(m)$$

where $\mathbf{w}_{[\mathbf{g}]_{i_1, i_2}}^{\kappa,k}(m)$ are coefficients of an expansion equivalent (that is, using the same basis) to the expansion valid for $h_{i_1, i_2, i_3}^{\kappa}(n, m)$. \square

Define

$$\mathbf{h}_{i,k,l}^{\kappa}(n, m) = [h_{i,k,l}^{\kappa}(n + L_1, m + L_1), \dots, \\ \times h_{i,k,l}^{\kappa}(n + L_2, m + L_2)]^T$$

and

$$\mathbf{y}_{i,l}^{\kappa}(n) = [y_{i,l}^{\kappa}(n + L_1), \dots, y_{i,l}^{\kappa}(n + L_2)]^T \\ \mathbf{n}_{i,l}^{\kappa}(n) = [n_{i,l}^{\kappa}(n + L_1), \dots, n_{i,l}^{\kappa}(n + L_2)]^T$$

so that (16) can be written

$$\mathbf{y}_{i,l}^{\kappa}(n) = \sum_{k=1}^K \sum_m \mathbf{h}_{i,k,l}^{\kappa}(n, m) a_k(n - m) + \mathbf{n}_{i,l}^{\kappa}(n) \quad (48)$$

or

$$\mathbf{y}(n) = \sum_{k=1}^K \sum_m \mathbf{h}_k(n, m) a_k(n - m) + \mathbf{n}(n) \quad (49)$$

where

$$\mathbf{y}(n) = [\mathbf{y}_{1,1}^1(n)^T, \dots, \mathbf{y}_{K,Q}^A(n)^T]^T \\ \mathbf{n}(n) = [\mathbf{n}_{1,1}^1(n)^T, \dots, \mathbf{n}_{K,Q}^A(n)^T]^T \\ \mathbf{h}_k(n, m) = [\mathbf{h}_{1,k,1}^1(n)^T, \dots, \mathbf{h}_{K,k,Q}^A(n)^T]^T.$$

Then, we can express (37) as

$$\hat{a}_k(n) = \mathbf{g}_k^H(n) \left[\sum_{k=1}^K \sum_m \mathbf{h}_k(n, m) a_k(n - m) + \mathbf{n}(n) \right] \quad (50)$$

where $\mathbf{g}_k^H(n)$ contains the weights $g_{i,l}^{\kappa,k}(n, m)$ properly organized. We can also write

$$\hat{a}_k(n) = \mathbf{g}_k^H(n) \left[\mathbf{h}_k(n, 0) a_k(n) \right. \\ \left. + \sum_{l=1, l \neq k}^K \sum_{m \neq 0} \mathbf{h}_k(n, m) a_l(n - m) + \mathbf{n}(n) \right] \\ = \mathbf{g}_k^H(n) [\mathbf{h}_k(n, 0) a_k(n) + \mathbf{b}_k(n) + \mathbf{n}(n)]. \quad (51)$$

The MMSE solution for $\mathbf{g}_k(n)$ [20], [25] is well approximated by

$$\mathbf{g}_k(n) = [\mathbf{h}_k(n, 0) \mathbf{h}_k(n, 0)^H + \mathbf{S}_k]^{-1} \mathbf{h}_k(n, 0) \\ = \frac{1}{1 + \mathbf{h}_k(n, 0)^H \mathbf{S}_k^{-1} \mathbf{h}_k(n, 0)} \mathbf{S}_k^{-1} \mathbf{h}_k(n, 0) \\ \simeq \mathbf{S}_k^{-1} \mathbf{h}_k(n, 0) \quad (52)$$

where $\mathbf{S}_k = E\{\mathbf{b}_k(n) \mathbf{b}_k(n)^H\} + E\{\mathbf{n}(n) \mathbf{n}(n)^H\}$, and where we have used the fact that the scaling factor $1 + \mathbf{h}_k(n, 0)^H \mathbf{S}_k^{-1} \mathbf{h}_k(n, 0)$ changes more slowly than $\mathbf{h}_k(n, 0)$. The expression in (52) is justified in [20] and is valid also for decision-feedback filters with some modifications. The approximation was proved asymptotically valid by experimental results and in fact used also in [25] to analyze the performance of multichannel decision-feedback equalizers.

\mathbf{S}_k in our CDMA system model is very close to a diagonal matrix in practice if $a_k(n)$ are i.i.d. symbols, the fading processes $h_{i_1, i_2, i_3}^{\kappa}(n, m)$ are assumed independent (across antennas and paths), and the PN codes used are assumed ideally uncorrelated with shifted replicas of themselves and different codes. Expression (52) makes evident that the dynamics of the linear time-varying filter $\mathbf{g}_k(n)$ are asymptotically equivalent (up to scale factors) to the variations of $\mathbf{h}_k(n, 0)$.

ACKNOWLEDGMENT

The author acknowledges several important comments and observations from the reviewers that have led to a significant improvement in the presentation of the paper. Many superb engineers at Watkins-Johnson contributed to the hardware experiments described in this paper. The technical support from L. Jugler, W. Tariq, M. Oh, A. Faheem, H. Fan, J. Tsay, L. Ruck, J. Taylor, G. Rowe, P. Floyd, B. Hiller, D. Woodruff, D. Bell, S. Wilbur, C. Welch, K. Burr, D. Litke, S. Shaffer, B. Goettsch, T. Dziwulski, T. Potter, P. Kline, J. Vucetic, J. Rugolo, R. Lober is gratefully acknowledged.

REFERENCES

- [1] P. A. Bello, "Characterization of randomly time variant linear channels," *IEEE Trans. Commun.*, vol. COM-11, pp. 360–393, Dec. 1963.
- [2] Q. Dai and E. Shweddyk, "Detection of bandlimited signals over frequency selective Rayleigh fading channels," *IEEE Trans. Commun.*, vol. 42, pp. 941–950, Mar. 1994.
- [3] G. D'Aria, F. Muratore, and V. Palestini, "Simulation and performance of the pan-European land mobile radio system," *IEEE Trans. Veh. Technol.*, vol. 41, pp. 177–189, Feb. 1992.
- [4] I. Daubechies, *Ten Lectures in Wavelets*. Philadelphia, PA: SIAM, 1992.
- [5] —, "Orthogonal bases of compactly supported wavelets," *Commun. Pure Appl. Math.*, vol. 41, pp. 909–996, 1988.
- [6] R. W. Dijkerman and R. R. Mazumdar, "Wavelet representations of stochastic processes and multiresolution stochastic models," *IEEE Trans. Signal Processing*, vol. 42, pp. 1640–1652, July 1994.
- [7] D. L. Donoho, "Unconditional bases are optimal bases for data compression and for statistical estimation," *Appl. Computat. Harmonic Anal.*, pp. 100–115, Dec. 1993.
- [8] D. L. Donoho, M. Vetterli, R. A. DeVore, and I. Daubechies, "Data compression and harmonic analysis," *IEEE Trans. Inform. Theory*, pp. 2435–2476, Oct. 1998.
- [9] G. B. Giannakis and C. Tepedelenlioglu, "Basis-expansion models and diversity techniques for blind identification and equalization of time-varying channels," *Proc. IEEE*, vol. 86, pp. 1969–1986, Oct. 1998.
- [10] P. Crespo and J. Jimenez, "Computer simulation of radio channels using harmonic decomposition techniques," *IEEE Trans. Veh. Technol.*, vol. 44, pp. 414–419, Aug. 1995.
- [11] M. I. Doroslovacki and H. Fan, "Wavelet-based linear system modeling and adaptive filtering," *IEEE Trans. Signal Processing*, vol. 44, pp. 1156–1167, May 1996.
- [12] W. C. Jakes Jr., *Microwave Mobile Communications*. New York: Wiley, 1974.
- [13] S. Verdu, *Multiuser Detection*. New York: Cambridge Univ. Press, 1998.
- [14] S. Mallat, "A theory for multiresolution signal decomposition the wavelet representation," *IEEE Trans. Pattern Anal. Machine Intell.*, vol. 11, pp. 674–693, July 1989.
- [15] M. Martone, "Wavelet-based separating kernels for sequence estimation with unknown rapidly time-varying channels," *IEEE Commun. Lett.*, vol. 3, pp. 78–80, Mar. 1999.
- [16] —, "An adaptive algorithm for adaptive antenna array low-rank processing in cellular TDMA base stations," *IEEE Trans. Commun.*, vol. 46, pp. 627–643, May 1998.
- [17] —, "On MMSE real-time antenna array processing using fourth-order statistics in the US cellular TDMA system," *IEEE J. Select. Areas Commun.*, vol. 16, pp. 1396–1410, Oct. 1998.
- [18] —, "Cumulant-based adaptive multi-channel filtering for wireless communication systems with multipath RF propagation using antenna arrays," *IEEE Trans. Veh. Technol.*, vol. 47, pp. 377–391, May 1998.
- [19] —, "Complex scaled tangent rotations (CSTAR) for fast space-time adaptive equalization of wireless TDMA," *IEEE Trans. Commun.*, vol. 46, pp. 1587–1591, Dec. 1998.
- [20] P. Monsen, "Theoretical and measured performance of a DFE modem on a fading multipath channel," *IEEE Trans. Commun.*, vol. 25, pp. 1144–1153, Oct. 1977.
- [21] J. G. Proakis, *Digital Communications*. New York: McGraw-Hill, 1989.
- [22] O. Rioul, "A discrete-time multiresolution theory," *IEEE Trans. Signal Processing*, vol. 41, pp. 2591–2606, Aug. 1993.
- [23] M. E. Rollins and S. J. Simmons, "Simplified per-survivor Kalman processing in fast frequency-selective fading channels," *IEEE Trans. Commun.*, vol. 45, pp. 544–553, May 1997.
- [24] L. L. Scharf, *Statistical Signal Processing*. Reading, MA: Addison-Wesley, 1991.
- [25] M. Stojanovic, J. G. Proakis, and J. A. Catipovic, "Analysis of the impact of channel estimation errors on the performance of a decision-feedback equalizer in fading multipath channels," *IEEE Trans. Commun.*, vol. 43, pp. 877–886, Feb./Mar./Apr. 1995.
- [26] M. K. Tsatsanis and G. B. Giannakis, "Time-varying system identification and model validation using wavelets," *IEEE Trans. Signal Processing*, vol. 41, pp. 3512–3523, Dec. 1993.
- [27] P. P. Vaidyanathan, *Multirate Systems and Filter Banks*. Englewood Cliffs, NJ: Prentice-Hall, 1993.
- [28] L. Van Trees, *Detection, Estimation, and Modulation Theory, Pt. I*. New York: Wiley, 1968.
- [29] H. Liu and M. D. Zoltowski, "Blind equalization in antenna array CDMA systems," *IEEE Trans. Signal Processing*, vol. 45, pp. 161–172, Jan. 1997.
- [30] P. Kline, T. Harris, and H. Anderson, "Wideband Base Station Architecture for Digital Communications System," US Patent no. 5 678 268. Filed July 19, 1995, Issued June 16, 1998.
- [31] J. Zhang and G. Walter, "A wavelet-based KL-like expansion for wide-sense stationary random processes," *IEEE Trans. Signal Processing*, vol. 42, pp. 1737–1745, July 1994.



Massimiliano (Max) Martone (M'93) was born in Rome, Italy. He received the "Doctor in Electronic Engineering" degree from the University of Rome "La Sapienza," Rome, Italy, in 1990.

From 1990 to 1991, he was with the Italian Air Force, and he consulted in the area of digital signal processing applied to communications for Staer, Inc., S.P.E., Inc., and TRS-Alfa Consult, Inc. In 1991, he joined the technical staff of the On-Board Equipment Division, Alenia Spazio, where he was involved in the design of satellite receivers and spread-spectrum transponders for the European Space Agency. From 1992 to 1994, he collaborated with the digital communications research group of Fondazione Ugo Bordoni. In 1994, he was appointed Visiting Scientist at the ECSE Department of Rensselaer Polytechnic Institute, Troy, NY. He was a wireless communications consultant for ATS, Inc., Waltham, MA, and in 1995, he joined the Telecommunications Group of Watkins-Johnson Company, Gaithersburg, MD, where he became Head of the Advanced Wireless Development section. In January 2000, he joined WJ Communications, Palo Alto, CA, as a Senior Staff Scientist to coordinate the development of new technologies for wireless broad-band access. He has been a leader in the development of several proprietary signal processing algorithms and digital hardware platforms used in Watkins-Johnson state-of-the-art wireless products. He has published more than 50 papers in international journals and proceedings of international conferences, and he has contributed to one book on cellular communications. He has been listed in Marquis Who's Who in the World, Who's Who in Finance in Industry, and Who's Who in the East. His main interests are in advanced signal processing for wireless receivers implementation, spread-spectrum multiple-access communications, cellular radio architectures, and VLSI implementations.

Dr. Martone is a Member of the the New York Academy of Sciences and the American Association for the Advancement of Science. He received 14 Watkins-Johnson Editorial Achievement Awards.